Somatic mutations of *GNA11* and *GNAQ* in *CTNNB1*-mutant aldosterone-producing adenomas presenting in puberty, pregnancy or menopause

Junhua Zhou https://orcid.org/0000-0002-8593-8393 [1,2,24], Elena AB Azizan https://orcid.org/0000-0002-5549-4242 [1,3,24*], Claudia P Cabrera[2,4,24], Fabio Fernandes-Rosa[5,24], Sheerazed Boulkroun[5,24], Giulia Argentesi[1,2], Emily Cottrell[6], Laurence Amar[5,7], Xilin Wu[1,2], Sam O'Toole[1,2], Emily Goodchild[1,2], Alison Marker[8], Russell Senanayake[9], Sumedha Garg[1,2,9], Tobias Åkerström, Samuel Backman[10], Suzanne Jordan[11], Satyamaanasa Polubothu[12], Dan Berney[13], Anna Gluck[14], Kate Lines[14], Rajesh V. Thakker https://orcid.org/0000-0002-1438-3220 [14], Antoinette Tuthill[15], Caroline Joyce[15], Juan Pablo Kaski[16], Fiona Karet Frankl[17], Lou Metherell[6], Ada Teo[18], Mark Gurnell[9], Laila Parvanta[19], William Drake[20], Eva Wozniak[2,21], David Klinzing[22], Jyn Ling Kuan[22], Zenia Tiang[22], Celso E. Gomez Sanchez https://orcid.org/0000-0002-9882-2082 [23], Per Hellman[10], Roger Foo[22], Chaz Mein[2,21], Veronica Kinsler[11], Peyman Bjorklund[10], Helen Storr[6,25], Maria-Christina Zennaro https://orcid.org/0000-0001-5449-9191 [5,25*], Morris J Brown https://orcid.org/0000-0001-8409-1082 [1,2,25*]

1. Endocrine Hypertension, Department of Clinical Pharmacology, William Harvey Research Institute, Queen Mary University of London, United Kingdom.
2. NIHR Barts Cardiovascular Biomedical Research Centre, Barts and The London School of Medicine and Dentistry, Queen Mary University of London, United Kingdom.
3. Department of Medicine, The National University of Malaysia (UKM) Medical Centre, Malaysia.
4. Centre for Translational Bioinformatics, William Harvey Research Institute, Queen Mary University of London, United Kingdom.
5. INSERM, U970, Paris Cardiovascular Research Center (PARCC), France.
6. Centre for Endocrinology, William Harvey Research Institute, Queen Mary University of London, United Kingdom.

7. Assistance Publique-Hôpitaux de Paris, Hôpital Européen Georges Pompidou, Unité Hypertension artérielle, France.
8. Department of Pathology, Addenbrookes Hospital, United Kingdom.
9. Metabolic Research Laboratories, Welcome Trust-MRC Institute of Metabolic Science, Cambridge Biomedical Campus, United Kingdom.
10. Department of Surgical Sciences, Uppsala University, Sweden.
11. Cellular Pathology Department, Royal London Hospital, United Kingdom.
12. Genetics and Genomic Medicine, University College London Great Ormond Street Institute of Child Health, United Kingdom.
13. Department of Molecular Oncology, Barts Cancer Institute, Queen Mary University of London, United Kingdom.
14. Academic Endocrine Unit, Radcliffe Department of Medicine, University of Oxford, United Kingdom.
15. Clinical Biochemistry, Cork University Hospital, Ireland.
16. Centre for Inherited Cardiovascular Diseases, Great Ormond Street Hospital and University College London Institute of Cardiovascular Science, London
17. Cambridge Institute for Medical Research, University of Cambridge, United Kingdom.
18. Dept of Medicine, Yong Loo Lin School of Medicine, National University of Singapore, Singapore.
19. Department of Surgery, Barts Hospital, United Kingdom.
20. Department of Endocrinology, Barts Hospital, United Kingdom.
21. Barts and London Genome Centre, School of Medicine and Dentistry, Blizard Institute, Queen Mary University of London, United Kingdom.
22. Cardiovascular Research Institute, Yong Loo Lin School of Medicine, National University of Singapore, Singapore.
23. G.V. (Sonny) Montgomery VA Medical Center and Department of Pharmacology and Toxicology, University of Mississippi Medical Center, United States of America.

24. These authors contributed equally.

25. These authors jointly supervised this work. *email: elena.azizan@ukm.edu.my; maria-christina.zennaro@inserm.fr; morris.brown@qmul.ac.uk

Abstract

Most aldosterone-producing adenomas (APA) have gain-of-function somatic mutations of ion-channels or transporters. However, their frequency in aldosterone-producing cell-clusters of normal adrenals suggests a requirement for co-driver mutations in APAs. Here we identified gain-of-function mutations in both CTNNB1 and GNA11 by whole exome sequencing of 3/41 APAs. Further sequencing of known CTNNB1-mutant APAs led to a total of 16 of 27 (59%) with a somatic p.Gln209His, p.Gln209Pro or p.Gln209Leu mutation of GNA11 or GNAQ. Solitary GNA11 mutations were found in hyperplastic zona glomerulosa adjacent to double-mutant APAs. Nine of ten patients in the UK/Irish cohort presented in puberty, pregnancy, or menopause. Among multiple transcripts upregulated >10-fold in double-mutant APAs was LHCGR, the receptor for luteinising or pregnancy hormone (human-chorionic-gonadotropin). Transfections of adrenocortical cells demonstrated additive effects of GNA11 and CTNNB1 mutations on aldosterone secretion and expression of genes upregulated in double-mutant APAs. In adrenal cortex, GNA11/Q mutation appears clinically silent without a co-driver mutation of CTNNB1.

Keywords: Adrenal gland diseases; Adrenal Tumours; Aldosterone; DNA sequencing; Primary Aldosteronism

Main

Primary aldosteronism (PA) is a major cause of hypertension. This is potentially curable when due to an aldosterone-producing adenoma (APA) in one adrenal. Conversely, when PA is overlooked, it leads to resistant hypertension and high cardiovascular risk. The landmark report in 2011 of somatic gain-of-function mutations in *KCNJ5* in 30-40% of APAs was followed by the discovery of further ion-channel or transporter mutations, mainly of *CACNA1D*, *ATP1A1* and *ATP2B3*, and of some clinical, pathological and biochemical differences between *KCNJ5*-mutant APAs and the others.[1-4] In particular, *KCNJ5*-mutant APAs are commoner in women, and have features resembling the cortisol-secreting cells of physiological zona fasciculata (ZF).[5-8] Conversely, APAs with other ion-channel mutations are commoner in men, and resemble the physiological smaller aldosterone-producing cells of adrenal zona glomerulosa (ZG).[4,9] Opinion has varied whether the residual 20-30% of APAs without apparent mutation is due to sampling from parts of an APA which do not express the aldosterone-synthesizing enzyme, CYP11B2, or to the existence of further somatic mutations yet to be discovered.[8-10] The genes whose mutation increases aldosterone production may differ from those responsible for tumour formation. Several of the former, particularly *CACNA1D,* are frequently mutated in the aldosterone-producing cell clusters (or nodules) of otherwise normal adrenals.[11] *KCNJ5* mutation was initially proposed to stimulate cell proliferation, as well as aldosterone production.[1] But the increased calcium entry consequent on mutation stimulates apoptosis rather than proliferation.[12] Wnt-activating mutations of *CTNNB1*, encoding β-catenin, are found in ~5% of APAs. β-catenin is a co-activator for a number of transcription factors, and mutations which prevent phosphorylation of exon-3 residues are regarded as oncogenic, in adrenal and other tumors.[8,10,13,14] However, there are only rare reports of *CTNNB1* mutations co-existing with somatic mutations which activate aldosterone production,[8,15] and in most APAs with *CTNNB1* mutations, these have been apparently solitary.[13,16] Whether *CTNNB1* mutations are able on their own to stimulate autonomous aldosterone production, or co-exist with other unidentified mutations, has not been resolved.

The three whole exome sequencing (WES) studies, which initially found *CACNA1D*, *ATP1A1*, and *ATP2B3* mutant *APAs*, [2-4] also reported several other genes mutated in the tumour DNA. However, even re-interrogation of the 3 WES studies together did not reveal additional potential pathogenic mutations that are present in more than one sample. We therefore undertook another WES of tumour and germline DNA from a new cohort of 41 patients in order to determine whether there are further genes with recurrent somatic mutation, and whether these were associated with a specific clinical or biochemical phenotype.

Results

Identification of pathogenic somatic mutations in APAs

WES found somatic mutations of the four ion-channel/transporter genes, at known hotspots, in 29 of the 41 APAs (**Supplementary Table 1**). Somatic mutations of *CACNA1D* were the most frequent *(n=11),* followed by *KCNJ5 (n=9)*, *ATP1A1 (n=5)* and *ATP2B3 (n=4).* Three APAs had a known mutation of *CTNNB1*. All three were noted to have a second mutation, of the Q209 residue of *GNA11,* which encodes the G-protein, G11. This, or the closely homologous Gq, mediates the aldosterone response to its principal physiological stimulus, angiotensin II (**Figure 1a**), and the highly conserved p.Gln209 residue is essential for GTPase activation (**Figure 1b**).[17,18] Mutations cause constitutive G11/q activation.

Sanger sequencing and replication of *GNA11/Q* genotype

UK/Ireland (discovery cohort): The p.Gln209His or p.Gln209Pro mutations of *GNA11* were found in the APAs of four further patients in whom presentation in periods of high LH/HCG had prompted discovery of somatic mutations in exon 3 of *CTNNB1* (**Supplementary Figure 1a**). One patient was indeed our index case of *CTNNB1* mutation, detected by our first WES, where the p.Gln209His mutation of *GNA11* was reported in the pair-wise comparison analysis.[4] Once we recognized the co-existence of mutations

in *CTNNB1* and *GNA11*, and associated features reported herein, targeted sequencing identified somatic exon 3 mutations of *CTNNB1* and p.Gln209 mutations of either *GNA11* or closely homologous *GNAQ* in 3 further APAs (**Supplementary Figure 1a**). Of the total cohort, one was a 12-year old boy presenting at puberty, and the other nine were women, with presentations in early pregnancy (n=7) or menopause (n=1). All ten were completely cured of hypertension post-adrenalectomy (**Table 1**).

French cohort: Mutation at p.Gln209 of either *GNA11* or *GNAQ* was sought in 13 APAs from patients in France. These APAs had previously undergone targeted sequencing, and been found to have somatic mutations at exon 3 of *CTNNB1.* Of these 13, three APAs had mutations at p.Gln209 of *GNA11* and one at p.Gln209 of *GNAQ* (**Table 2** and **Supplementary Figure 1b**). During the study, double-mutation was suspected in a fifth woman, aged 17, whose PA dated from puberty; her APA was confirmed to have somatic mutation at p.Gly34 of *CTNNB1* and p.Gln209 of *GNAQ* (**Table 2** and **Supplementary Figure 1b**). As controls, a further nine APAs with known ion-channel/transporter gene mutations, but no mutation of *CTNNB1*, were genotyped. In none of these nine cases was a mutation found in *GNA11* or *GNAQ*.

Swedish cohort: Further replication was achieved by re-analysis of the RNAseq FASTQ data from the APAs of a published cohort of 15 Swedish patients.[19] This included 3 APAs with somatic mutations of *CTNNB1.* The re-analysis found one of these to have a p.Gln209His mutation of *GNAQ* (**Table 2**). No mutation of *GNA11* or *GNAQ* was seen in the other 12 APAs that had one of the known ion-channel/transporter gene mutations. [19]

In summary, 23/27 patients with *CTNNB1*-mutant APAs were women. 16 of the 27 (59%) had a mutation at p.Gln209 of *GNA11* (n=11) or *GNAQ* (n=5). All were women except for the pubertal boy.

Functional analyses of *GNA11/Q* in human adrenocortical cells

H295R is an immortalised adrenocortical cell line heterozygous for the p.Ser45Pro mutation of *CTNNB1* but wild-type for *GNA11* (**Supplementary Figure 2a**). Transfection of H295R cells by each of

the *GNA11* mutations (**Supplementary Figure 2b**) increased aldosterone secretion and *CYP11B2* expression (encoding aldosterone synthase) by 4.0-6.2-fold and 3.4-4.2-fold respectively, compared to wild-type transfected cells (**Figure 2a-b**). The stimulatory effect of angiotensin II 10 nM was retained in the mutant-transfected cells (**Supplementary Figure 2c**). The stimulation of cortisol production by the mutations was less than of aldosterone (**Supplementary Figure 2d-e**). In order to determine whether the Q209 mutations of *GNA11* stimulate aldosterone production, even in the absence of CTNNB1 activation, the transfections of H295R cells were repeated after either silencing of CTNNB1 using a Dharmacon SMARTpool SiRNAs, or 24-h treatment with the CTNNB1 inhibitor, ICG-001.[20,21] Both interventions reduced the aldosterone production relative to vehicle-treated cells, as anticipated by published experiments (**Figure 2c-d)**.[22,23] However, neither silencing of CTNNB1 nor ICG-001 blunted the fold-increase in aldosterone secretion seen in mutant-transfected cells compared to wild-type (**Figure 2c-d and Supplementary Figure 2f**). As a further test whether *GNA11* mutations require co-existing *CTNNB1* activation in order to increase aldosterone production, we used primary adrenocortical cells freshly dispersed from aldosterone-producing adenomas, with wild-type genotype for *CTNNB1* and *GNA11* (**Supplementary Table 2**). Cells were transfected with one each of the *CTNNB1* and *GNA11* mutants, or with both mutants together, and compared with cells transfected with vector or wild-type genes. Aldosterone secretion and CYP11B2 expression were increased by the individual mutations, but their combination caused substantially greater increases (**Figure 2e** and **Supplementary Figure 2g**). We also studied the p.Gln290His mutation of *GNAQ.* Its transfection into H295R cells increased aldosterone secretion by 1.93-fold (sem = 0.06) (**Figure 2f).**

Biochemical phenotype of APAs with double mutations

LHCGR expression: We previously linked the presentation of the first three women at times of high circulating LH or HCG to high LHCGR expression by *CTNNB1*-mutant APAs.[16] To determine whether the association requires double-mutation of *CTNNB1* and *GNA11,* rather than *CTNNB1* mutation alone, we performed qPCR of *LHCGR* in all *CTNNB1*-mutant APAs from the 3 cohorts. Fold-changes >10

(compared to available controls for each cohort) were seen in 15/16 double-mutant APAs (**Figure 3a-c**). The exception, patient 10, was the sole patient with a p.Gln209Leu mutation. Of possible note, her adrenalectomy coincided with menstruation, when LHCGR expression, at least in ovarian follicles, is suppressed to <10% of maximum.[24] 7/9 single-mutant APAs had low or undetectable *LHCGR* mRNA (*P*=0.0001, Fisher exact test).

APAs from the ten UK/Irish patients were positive for LHCGR on immunohistochemistry (IHC) (**Figure 3d** and **Supplementary Figure 3a**). Expression within APAs was variable, particularly in APAs with variable expression of CYP11B2. In the APA from patient 10, which had low mRNA expression for LHCGR, the protein was concentrated in a visually distinct segment; this allowed demonstration that variation in IHC signal corresponded to fold-change on qPCR (**Supplementary Figure 3a).** Adrenal medulla was also unexpectedly positive, confirmed by analyses of laser-capture microdissected RNA (**Supplementary Figure 3b**). Since LHCGR in steroidogenic cells is coupled to both GαS and GαQ/11, the consequences of activation will depend not only on LH/HCG levels, but on downstream signalling, and paracrine stimulation by other cell-types with physiological expression of LHCGR.[25] There was also striking heterogeneity in subcellular sites of expression (**Supplementary Figure 3c**). Membranous and vesicular expression were commonest in double mutant APAs, but cytosolic in adjacent ZG (**Supplementary Figure 3d**).

There is no expression of LHCGR in H295R cells, indicating that LH/HCG stimulation is not essential in these cells to the induction of autonomous aldosterone production by *GNA11/Q* mutation (**Supplementary Figure 3e** and **Figure 2a-b,f**). The steroidome of H295R cells suggests a cell of origin in zona reticularis, far downstream of the primordial adrenogenital cells that are the common precursor of gonads and adrenal cortex.[26] We therefore turned again to primary adrenocortical cells, comparing LHCGR expression in cells transfected with mutant GNA11 and CTNNB1, alone or together. qPCR showed greater expression of *LHCGR* in cells transfected with mutations of both genes, than with single-mutations or vector (**Figure 3e).** The low transfection of primary cells also enabled

comparisons of individual cells, by immunofluorescence, both within and between each well. The red immunofluorescence for LHCGR was qualitatively intense, and frequently membranous, in cells positive for both mutations, but was scarce in GFP-negative cells lacking *GNA11* p.Gln209 mutation (**Figure 3f and Supplementary Figure 3e-i).** Quantitative analysis confirmed a higher LHCGR intensity in cells with *GNA11*-mutant transfection (**Figure 3g)**. However some *GNA11*-mutant cells were LHCGR positive even without *CTNNB1* transfection. Post-hoc analysis showed that LHCGR (red) intensity was qualitatively and quantitatively associated with immunofluorescence (magenta) for CTNNB1 (**Supplementary Figure 3j)**, consistent with adrenocortical Wnt activation in PA.[27,28] When both plasmids were transfected into primary adrenocortical cells, and these were compared by intensity of green (GNA11) and magenta (CTNNB1), the red (LHCGR) intensity was 31-144 fold higher in cells with GNA11-p.Gln209Pro transfection and high CTNNB1 intensity, than in other cells (**Extended Data Figure 1**).

Expression of top differentiated genes: LHCGR was the most upregulated gene (compared to other APAs in the same microarray) in the APA of patient 4,[16] but a weaker pregnancy association in the replication cohorts (**Table 1** and **Table 2**) prompted us to ask whether there are other genes consistently upregulated in the double-mutant APAs. We re-examined our previous public-domain expression data (microarray or RNA seq) performed in three of the double-mutant APAs before their genotype was known: the index case from 2013 (patient 4)[4,29,30]; the APA from a menopausal woman (patient 6)[5]; and the newly diagnosed Swedish double mutant APA (S1)[19]. Unsupervised hierarchical clustering analysis of the most variably expressed genes in the 3 studies showed clustering of the 3 double-mutant APAs, and a high proportion of genes were many-fold upregulated compared to other APAs (**Figure 4a**). *LHCGR* is among several 'hallmark' genes with uniquely high expression in the 3 double-mutant APAs, including the neuronal cell adhesion molecule, *TMEM132E,* and Wnt inhibitor, *DKK1* (**Figure 4b**). Further genes are upregulated also in other ZG-like (compared to *KCNJ5*-mutant) APAs, or in one or both solitary *CTNNB1*-mutant APAs. A small number of genes are down-regulated

in the double-mutant APAs, including CYP11B1 (**Figure 4b**). This gene encodes the final enzyme in cortisol synthesis (11 b-hydroxylase). Enrichment analysis using DAVID (Database for Annotation, Visualization and Integrated Discovery v6.8) showed significant enrichment of features or terms concerned with cell-junction/cell adhesion or synapse (**Supplementary Table 3**).

qPCR confirmed large (~10 to 1000-fold) higher expression of several of the hallmark transcripts in 4-5 double-mutants (from whom RNA of fresh-frozen tissue remained) than in 9 matched APAs without mutations of either gene (**Figure 4c-d**), or (for TMEM132E) than in 7 APAs with solitary mutation of *CTNNB1* (**Figure 4e**). However, qPCR of H295R cells (with germline S45P mutation of *CTNNB1*) transfected with mutant *GNA11* showed only *TMEM132E*, of the 6 tested genes, to be substantially upregulated (**Figure 4f**). *TMEM132E*, and *LHCGR*, were the top genes that differed most robustly between double-mutant and other APAs, including those with solitary mutations of *CTNNB1* (**Figure 4e** and **Supplementary Figure 4**). LHCGR itself remained undetectable after transfection of mutant *GNA11*.

In a previous IHC analysis of eight *CTNNB1*-mutant APAs, we reported four with low CYP11B2 (H-score <30) and high CYP11B1 expression (H-score >200), versus three with high CYP11B2 (H-score>200) and low CYP11B1 expression (H-score <1).[14] No genotyping was available from these patients. But IHC in two of the current Swedish cohort showed similar contrast between the single- and double-mutant (**Supplementary Figure 5a**), supported by qPCR and aldosterone measurements (**Supplementary Figure 5b)**. These findings, and the low CYP11B1 expression highlighted in the heatmap of the 3 double-mutant APAs (**Figure 4b**), prompted us to analyse *CYP11B1* and *CYP11B2* expression in double mutant APAs compared to APAs with single mutations of *CTNNB1* or other genotypes. qPCR confirmed a low CYP11B1/CYP11B2 ratio, and an overall low expression of CYP11B1, in ten double-mutant APAs with available RNA (**Figure 5a**). IHC of all the UK/Irish double-mutant APAs, showed absent CYP11B1 but strong staining of CYP11B2 (**Figure 5b).**

Phenotype and genotype of adjacent adrenals

The IHC also showed consistent hyperplasia of adjacent ZG, with absence of both CYP11B1 and CYP11B2 staining, but weak/moderate staining for LHCGR (**Supplementary Figure 5c)**. There were few aldosterone-producing cell clusters (APCCs), and a possible atrophy of zona fasciculata (ZF). The ZG expansion resembles that in mice with transgenic activation of adrenal Gq or CTNNB1.[31,32] A similar picture is also seen in a minority of patients with mosaicism of *GNAS* at the residues analogous to the p.Gln209 or p.Arg183 residues of *GNA11/Q* (McCune Albright syndrome).[33-35] We therefore wondered whether loci of *GNA11* mutation may be present in the adrenal cortex adjacent to APAs with *GNA11* mutations at p.Gln209.

Multiple punch biopsies were taken, for gDNA (± cDNA sequencing and qPCR) from 6 regions of fresh-frozen adrenal available from patient 7 (**Figure 6a-c**). gDNA from 3 regions had the same double-mutation genotype as the original tumor (**Supplementary Figure 6a(i)**); in one case the associated cDNA had low expression of CYP11B2 and LHCGR **(Figure 6b).** Samples from the other three regions were *CTNNB1*-wild type but one (DNA1) had the same p.Gln209His mutation of *GNA11* as the APA, homozygous in R1 gDNA and heterozygous in R1 cDNA (**Supplementary Figure 6a(i)** and **Figure 6c**). The latter had undetectable levels of *CYP11B2*, *LHCGR* (**Figure 6b**) and other hallmark differentially expressed genes (DEG) high in double mutant APAs (**Supplementary Figure 6a(ii)**), confirming its separation from the APA. In patient 6, a focal area of peri-medullary ZG cells was weakly positive for CYP11B2 (Extended Data **Figure 2a)** and for mutations of *GNA11* and *CTNNB1* (Extended Data **Figure 2b-c**). qPCR from this double-mutant region showed intermediate expression of several DEG genes (Extended Data **Figure 2d).** For more precise analysis and location, we undertook laser capture microdissection (LCM) of a formalin-fixed paraffin embedded adrenal section from patient 1, in which ZG was intact in the adjacent adrenal gland (**Figure 6d-e**). Two of eight sites (ZG1 and ZG6) at distinct ends of the adrenal limbs were, respectively, heterozygous or homozygous for the same p.Gln209Pro mutation in *GNA11* as the APA, but did not have the APA's mutation of *CTNNB1* (**Figure 6f** and

Supplementary Figure 6b). The findings of APA mutations in adjacent adrenal were replicated in each case by up to 3 quantitative techniques (ddPCR for *GNA11* and *GNAQ*, targeted NGS for both tumor genes, and WES) (**Supplementary Table 4a-d).** There was high concordance between ddPCR, NGS and Sanger sequencing when analyzed in the same sample, e.g. in patient 6 (**Figure 5Bii-iii and Supplementary Table 4a)**. Where fresh samples were re-taken, concordance with Sanger sequencing was lower, e.g. patient 1 (**Figure 6d-f and Supplementary Table 4b)** and patient 7 (**Supplementary Table 4a-b**), and NGS detected both tumor genes in some samples. Minor allele frequencies (MAF) >3% were not seen for other bases in the targeted region, or at the same base in other adrenals. No mutations were found in 4 adrenals adjacent to APAs with *KCNJ5* or *CACNA1D* mutations (**Supplementary Table 4d)**, nor in a limited number of scrapings adjacent to the double-mutant APAs from patients 2, 8, and 9 (**Supplementary Table 4b-c).**

In McCune Albright mutation can be difficult to detect, and appear homozygous, heterozygous or absent at adjacent sites.[36,37] Finding an APA's mutation at disparate sites of adjacent ZG could point to an origin during adrenogenesis, but strictly defined mosaicism is hard to prove within single tissues.

Discussion

We report the discovery of gain-of-function mutations of the G-protein, *GNA11,* or its close homologue, *GNAQ*, in multiple APAs. To date, the mutation is always residue p.Gln209, and associated with a gain-of-function mutation of *CTNNB1.* Mutation of p.Gln209, or homologous p.Gln in GNAS, GNA12-14, impair hydrogen bonds between G-protein α and β subunits.[17,18] In ZG, Gq/11 mediate the aldosterone response to angiotensin II, via stimulation of intracellular Ca^{2+} release by inositol trisphosphate (IP3).[38] From 2009, somatic mutations of the Gln209 or Arg183 codons of *GNA11* or *GNAQ* were reported in the majority of uveal melanomas, and in several congenital skin or vascular lesions, including blue nevi and Sturge Weber syndrome.[39-41] In some congenital lesions, the mutation of GNA11/Q is mosaic, being found in several disparate sites.[42]

The role of Wnt signalling in adrenal development, and APA formation, is well established.[28,43,44] Usually the Wnt activation in APAs is present without mutation of *CTNNB1,* but gain-of-function somatic mutations of exon 3 of *CTNNB1* are found in ~5% of APAs, as well as other adrenal tumours.[10,13,14,27,45,46] 20-30% of malignant adrenocarcinomas of the adrenal (ACC) have the same mutations of *CTNNB1* as occur in APAs;[27] but mutations of *GNA11/Q* are absent from ACCs, and their common co-driver mutations are in different genes (e.g. *TP53, MED12)*.[47] In many malignancies, co-drivers are the exception, often following chemotherapy.[48,49]

So why do our two well-known oncogenic mutations cluster in APAs, but seemingly no other tumour? Occasional APAs have been reported with dual mutation of *CTNNB1* and *CACNA1D*.[50] However, unlike GNA11/Q, *CACNA1D* appears to be the sole driver in most APAs where it is mutated, or to co-exist with such a variety of mutations that no other gene was recurrently co-mutated in our 11 *CACNA1D*-mutant APAs. The greater prevalence of *CTNNB1* than *GNA11/Q* mutations, and the ZG hyperplasia of mice with *CTNNB1* mutations, might suggest that *GNA11/Q* mutations arise in a subset of *CTNNB1*-mutant APAs[51]. In possible support, Wnt activation by germline mutation of *APC* predisposes, rarely, to somatic mutation of *KCNJ5.*[52] In possible opposition is the high CYP11B1 expression of solitary *CTNNB1*-mutant APAs, but exceptionally low expression in the double-mutants, suggesting different sites of origin within the adrenal cortex.

The clue to whether one mutation generally precedes the other may come from growing evidence that increased transcription drives mutation,[53] and from examples where Gq/11 lie upstream of CTNNB1 activation. As proof-of-concept, mutation of upstream *MAPK* in the melanogenesis pathway leads via second-hit mutation of *CTNNB1* to penetrating nevi.[54] A recent study of p.Gln209 mutations of *GNAQ* in uveal melanoma suggested that these cause hyperplasia, 'being insufficient for neoplastic transformation', and highlighted clustering of driver mutations within KEGG pathways to explain recurrent second hits.[55] Coincidentally, GNA11/Q and CTNNB1 feature together in just one KEGG pathway, melanogenesis. Adrenal MC1R expression, and presence of melanin in occasional pigmented

adrenal nodules, seem unlikely to be directly relevant to our double-mutant APAs [56,57]. But the connection between *GNAQ* and *CTNNB1* in melanogenesis is the Wnt receptor, FZD6, which is the most upregulated frizzled in ZG.[29] An additional potential link between Gq/11 and *CTNNB1* activation is through RSPO3.[58] The RSPO3-LGR5 pathway is active in ZG, maybe controlling cell proliferation and migration as in intestinal crypts.[29,59-61] In summary, *GNA11/Q* mutations may arise early and create conditions in which a second hit in *CTNNB1* leads to APA formation. Proven examples of *GNA11/Q* mosaicism, and the disconnected, discrete areas of *GNA11* mutation in adjacent hyperplastic ZG, are consistent with this view.[42] *CTNNB1* mosaicism has occasionally been suggested, and much further work is required to determine whether mosaicism for either or both genes might be the antecedent to double-mutant APAs.[62,63] A case of KCNJ5 mosaicism was recently reported.[64]

In the replication cohorts from France and Sweden, single-mutant outnumbered double-mutant APAs by 2:1, whereas no single-mutant APAs were found among UK patients. The latter came from a variety of endocrine, renal and hypertension clinics, with no apparent referral bias. Ethnic variation in somatic mutation of several genes is recognised in APAs, with *KCNJ5* mutations being commoner in Oriental than Caucasian cohorts, and less frequent than *CACNA1D* in Black patients, in whom no *CTNNB1* mutations are yet reported.[50,65] Ethnic variation within Europe may seem less likely than between continents. Although melanogenesis is probably irrelevant to adrenal p.Gln209 mutation, *MC1R* genotype and phenotype (red hair) illustrate intra-continental heterogeneity.[66]

Our findings suggest that onset of hypertension in the first trimester – the period of peak HCG secretion – should prompt consideration of PA. Most pregnancy-associated hypertension arises in later trimesters. The index case of our original report was successfully managed on amiloride through pregnancy, whereas undiagnosed PA is high-risk for mother and fetus.[16,67] We previously linked the seemingly explosive presentation of *CTNNB1*-mutant APAs in early pregnancy to their induction of LHCGR expression. We have not ourselves confirmed LH responsiveness of cells transfected with mutant CTNNB1 and GNA11; but LH can induce the CYP11B2 promoter by 25-fold, in adrenocortical

cells transfected with LHCGR expression.[16,68] LH stimulates modest increases in aldosterone secretion in some patients with PA, and LHCGR is indeed commonly expressed in APAs and adjacent adrenal – though at a much lower level than in our *CTNNB1*-mutant APAs presenting in pregnancy.[16,69,70] Subsequently it became apparent that *CTNNB1* mutation was usually insufficient to cause the phenotype of LH/HCG-dependent PA.[69,71,72] Our finding of a second driver mutation explains much of the discrepant experience. Although the APA transcriptomes, and transfections of primary cells, show some overlap between phenotypes of single- and double-mutation, we infer that a double-hit within related pathways is more likely than a single-hit to cause large increases in expression of LHCGR, and of other genes which may influence clinical presentation.

References

1. Choi, M. *et al.* K+ channel mutations in adrenal aldosterone-producing adenomas and hereditary hypertension. *Science* **331**, 768-72 (2011).
2. Beuschlein, F. *et al.* Somatic mutations in ATP1A1 and ATP2B3 lead to aldosterone-producing adenomas and secondary hypertension. *Nat Genet* **45**, 440-444 (2013).
3. Scholl, U.I. *et al.* Somatic and germline CACNA1D calcium channel mutations in aldosterone-producing adenomas and primary aldosteronism. *Nat Genet* (2013).
4. Azizan, E.A. *et al.* Somatic mutations in ATP1A1 and CACNA1D underlie a common subtype of adrenal hypertension. *Nat Genet* **45**, 1055-60 (2013).
5. Azizan, E.A. *et al.* Microarray, qPCR and KCNJ5 sequencing of aldosterone-producing adenomas reveal differences in genotype and phenotype between zona glomerulosa- and zona fasciculata-like tumors. *J Clin Endocrinol Metab* **97**, E819-29 (2012).
6. Monticone, S. *et al.* Immunohistochemical, genetic and clinical characterization of sporadic aldosterone-producing adenomas. *Mol Cell Endocrinol* **411**, 146-54 (2015).
7. Akerstrom, T. *et al.* Novel somatic mutations and distinct molecular signature in aldosterone-producing adenomas. *Endocr Relat Cancer* **22**, 735-44 (2015).
8. De Sousa, K. *et al.* Genetic, Cellular, and Molecular Heterogeneity in Adrenals With Aldosterone-Producing Adenoma. *Hypertension* **75**, 1034-1044 (2020).
9. Nanba, K. *et al.* Targeted Molecular Characterization of Aldosterone-Producing Adenomas in White Americans. *J Clin Endocrinol Metab* **103**, 3869-3876 (2018).
10. Wu, V.C. *et al.* The prevalence of CTNNB1 mutations in primary aldosteronism and consequences for clinical outcomes. *Sci Rep* **7**, 39121 (2017).
11. Nishimoto, K. *et al.* Aldosterone-stimulating somatic gene mutations are common in normal adrenal glands. *Proc Natl Acad Sci U S A* **112**, E4591-9 (2015).
12. Williams, T.A. *et al.* Visinin-Like 1 Is Upregulated in Aldosterone-Producing Adenomas With KCNJ5 Mutations and Protects From Calcium-Induced Apoptosis. *Hypertension* **59**, 833-9 (2012).
13. Akerstrom, T. *et al.* Activating mutations in CTNNB1 in aldosterone producing adenomas. *Sci Rep* **6**, 19546 (2016).
14. Tadjine, M., Lampron, A., Ouadi, L. & Bourdeau, I. Frequent mutations of beta-catenin gene in sporadic secreting adrenocortical adenomas. *Clin Endocrinol (Oxf)* **68**, 264-70 (2008).
15. Omata, K. *et al.* Cellular and Genetic Causes of Idiopathic Hyperaldosteronism. *Hypertension* **72**, 874-880 (2018).
16. Teo, A.E. *et al.* Pregnancy, Primary Aldosteronism, and Adrenal CTNNB1 Mutations. *N Engl J Med* **373**, 1429-36 (2015).
17. Kalinec, G., Nazarali, A.J., Hermouet, S., Xu, N. & Gutkind, J.S. Mutated alpha subunit of the Gq protein induces malignant transformation in NIH 3T3 cells. *Mol Cell Biol* **12**, 4687-93 (1992).
18. Gutowski, S. *et al.* Antibodies to the alpha q subfamily of guanine nucleotide-binding regulatory protein alpha subunits attenuate activation of phosphatidylinositol 4,5-bisphosphate hydrolysis by hormones. *J Biol Chem* **266**, 20519-24 (1991).
19. Backman, S. *et al.* RNA Sequencing Provides Novel Insights into the Transcriptome of Aldosterone Producing Adenomas. *Sci Rep* **9**, 6269 (2019).
20. Wiese, M. *et al.* The beta-catenin/CBP-antagonist ICG-001 inhibits pediatric glioma tumorigenicity in a Wnt-independent manner. *Oncotarget* **8**, 27300-27313 (2017).
21. Zhou, L. *et al.* Multiple genes of the renin-angiotensin system are novel targets of Wnt/beta-catenin signaling. *J Am Soc Nephrol* **26**, 107-20 (2015).
22. Doghman, M., Cazareth, J. & Lalli, E. The T cell factor/beta-catenin antagonist PKF115-584 inhibits proliferation of adrenocortical carcinoma cells. *J Clin Endocrinol Metab* **93**, 3222-5 (2008).

23. Zhou, T. *et al.* CTNNB1 Knockdown Inhibits Cell Proliferation and Aldosterone Secretion Through Inhibiting Wnt/beta-Catenin Signaling in H295R Cells. *Technol Cancer Res Treat* **19**, 1533033820979685 (2020).
24. Jeppesen, J.V. *et al.* LH-receptor gene expression in human granulosa and cumulus cells from antral and preovulatory follicles. *J Clin Endocrinol Metab* **97**, E1524-31 (2012).
25. Breen, S.M. *et al.* Ovulation involves the luteinizing hormone-dependent activation of G(q/11) in granulosa cells. *Mol Endocrinol* **27**, 1483-91 (2013).
26. Gazdar, A.F. *et al.* Establishment and characterization of a human adrenocortical carcinoma cell line that expresses multiple pathways of steroid biosynthesis. *Cancer Res* **50**, 5488-96 (1990).
27. Tissier, F. *et al.* Mutations of beta-catenin in adrenocortical tumors: activation of the Wnt signaling pathway is a frequent event in both benign and malignant adrenocortical tumors. *Cancer Res* **65**, 7622-7 (2005).
28. Boulkroun, S. *et al.* Aldosterone-producing adenoma formation in the adrenal cortex involves expression of stem/progenitor cell markers. *Endocrinology* **152**, 4753-63 (2011).
29. Shaikh, L.H. *et al.* LGR5 Activates Noncanonical Wnt Signaling and Inhibits Aldosterone Production in the Human Adrenal. *J Clin Endocrinol Metab* **100**, E836-44 (2015).
30. Zhou, J. *et al.* Transcriptome Pathway Analysis of Pathological and Physiological Aldosterone-Producing Human Tissues. *Hypertension* **68**, 1424-1431 (2016).
31. Taylor, M.J. *et al.* Chemogenetic activation of adrenocortical Gq signaling causes hyperaldosteronism and disrupts functional zonation. *J Clin Invest* (2019).
32. Leng, S. *et al.* beta-Catenin and FGFR2 regulate postnatal rosette-based adrenocortical morphogenesis. *Nat Commun* **11**, 1680 (2020).
33. Schwindinger, W.F., Francomano, C.A. & Levine, M.A. Identification of a mutation in the gene encoding the alpha subunit of the stimulatory G protein of adenylyl cyclase in McCune-Albright syndrome. *Proc Natl Acad Sci U S A* **89**, 5152-6 (1992).
34. Weinstein, L.S. *et al.* Activating mutations of the stimulatory G protein in the McCune-Albright syndrome. *N Engl J Med* **325**, 1688-95 (1991).
35. Idowu, B.D. *et al.* A sensitive mutation-specific screening technique for GNAS1 mutations in cases of fibrous dysplasia: the first report of a codon 227 mutation in bone. *Histopathology* **50**, 691-704 (2007).
36. Vasilev, V. *et al.* McCune-Albright syndrome: a detailed pathological and genetic analysis of disease effects in an adult patient. *J Clin Endocrinol Metab* **99**, E2029-38 (2014).
37. Rey, R.A. *et al.* Unexpected mosaicism of R201H-GNAS1 mutant-bearing cells in the testes underlie macro-orchidism without sexual precocity in McCune-Albright syndrome. *Hum Mol Genet* **15**, 3538-43 (2006).
38. Wu, D.Q., Lee, C.H., Rhee, S.G. & Simon, M.I. Activation of phospholipase C by the alpha subunits of the Gq and G11 proteins in transfected Cos-7 cells. *J Biol Chem* **267**, 1811-7 (1992).
39. Ayturk, U.M. *et al.* Somatic Activating Mutations in GNAQ and GNA11 Are Associated with Congenital Hemangioma. *Am J Hum Genet* **98**, 789-95 (2016).
40. Van Raamsdonk, C.D. *et al.* Mutations in GNA11 in uveal melanoma. *N Engl J Med* **363**, 2191-9 (2010).
41. Shirley, M.D. *et al.* Sturge-Weber syndrome and port-wine stains caused by somatic mutation in GNAQ. *N Engl J Med* **368**, 1971-9 (2013).
42. Thomas, A.C. *et al.* Mosaic Activating Mutations in GNA11 and GNAQ Are Associated with Phakomatosis Pigmentovascularis and Extensive Dermal Melanocytosis. *J Invest Dermatol* **136**, 770-8 (2016).
43. Simon, D.P. & Hammer, G.D. Adrenocortical stem and progenitor cells: implications for adrenocortical carcinoma. *Mol Cell Endocrinol* **351**, 2-11 (2012).

44. Berthon, A. *et al.* WNT/beta-catenin signalling is activated in aldosterone-producing adenomas and controls aldosterone production. *Hum Mol Genet* **23**, 889-905 (2014).
45. Lerario, A.M., Moraitis, A. & Hammer, G.D. Genetics and epigenetics of adrenocortical tumors. *Mol Cell Endocrinol* **386**, 67-84 (2014).
46. Wang, J.J., Peng, K.Y., Wu, V.C., Tseng, F.Y. & Wu, K.D. CTNNB1 Mutation in Aldosterone Producing Adenoma. *Endocrinol Metab (Seoul)* **32**, 332-338 (2017).
47. Assie, G. *et al.* Integrated genomic characterization of adrenocortical carcinoma. *Nat Genet* **46**, 607-12 (2014).
48. Jakobsen, J.N., Santoni-Rugiu, E., Grauslund, M., Melchior, L. & Sorensen, J.B. Concomitant driver mutations in advanced EGFR-mutated non-small-cell lung cancer and their impact on erlotinib treatment. *Oncotarget* **9**, 26195-26208 (2018).
49. Gainor, J.F. *et al.* ALK rearrangements are mutually exclusive with mutations in EGFR or KRAS: an analysis of 1,683 patients with non-small cell lung cancer. *Clin Cancer Res* **19**, 4273-81 (2013).
50. Nanba, K. *et al.* Genetic Characteristics of Aldosterone-Producing Adenomas in Blacks. *Hypertension* **73**, 885-892 (2019).
51. Pignatti, E. *et al.* Beta-Catenin Causes Adrenal Hyperplasia by Blocking Zonal Transdifferentiation. *Cell Rep* **31**, 107524 (2020).
52. Vouillarmet, J. *et al.* Aldosterone-Producing Adenoma With a Somatic KCNJ5 Mutation Revealing APC-Dependent Familial Adenomatous Polyposis. *J Clin Endocrinol Metab* **101**, 3874-3878 (2016).
53. Polak, P. *et al.* Cell-of-origin chromatin organization shapes the mutational landscape of cancer. *Nature* **518**, 360-364 (2015).
54. Yeh, I. *et al.* Combined activation of MAP kinase pathway and beta-catenin signaling cause deep penetrating nevi. *Nat Commun* **8**, 644 (2017).
55. Piaggio, F. *et al.* Secondary Somatic Mutations in G-Protein-Related Pathways and Mutation Signatures in Uveal Melanoma. *Cancers (Basel)* **11**(2019).
56. Chen, X. *et al.* The melanoma-linked "redhead" MC1R influences dopaminergic neuron survival. *Ann Neurol* **81**, 395-406 (2017).
57. Cavlan, D., Storr, H.L., Berney, D., Evagora, C. & King, P.J. Adrenal pigmentation in PPNAD is a result of melanin deposition and associated with upregulation of the melanocortin 1 receptor. *Endocrine Abstracts* **38**, 154 (2015).
58. Binder, J.X. *et al.* COMPARTMENTS: unification and visualization of protein subcellular localization evidence. *Database (Oxford)* **2014**, bau012 (2014).
59. de Lau, W. *et al.* Lgr5 homologues associate with Wnt receptors and mediate R-spondin signalling. *Nature* **476**, 293-7 (2011).
60. Vidal, V. *et al.* The adrenal capsule is a signaling center controlling cell renewal and zonation through Rspo3. *Genes Dev* **30**, 1389-94 (2016).
61. Yi, H., Wang, Y., Kavallaris, M. & Wang, J.Y. Lgr4-Mediated Potentiation Of Wnt/β-Catenin Signaling Promotes MLL Leukemogenesis Via An Rspo3/Wnt3a-Gnaq Pathway In Leukemic Stem Cells. *Blood* **122**, 887 (2013).
62. Carter, J.M. *et al.* CTNNB1 Mutations and Estrogen Receptor Expression in Neuromuscular Choristoma and Its Associated Fibromatosis. *Am J Surg Pathol* **40**, 1368-74 (2016).
63. Crago, A.M. *et al.* Near universal detection of alterations in CTNNB1 and Wnt pathway regulators in desmoid-type fibromatosis by whole-exome sequencing and genomic analysis. *Genes Chromosomes Cancer* **54**, 606-15 (2015).
64. Maria, A.G. *et al.* Mosaicism for KCNJ5 Causing Early-Onset Primary Aldosteronism due to Bilateral Adrenocortical Hyperplasia. *Am J Hypertens* **33**, 124-130 (2020).
65. Zhang, E.D. *et al.* Mutation spectrum in GNAQ and GNA11 in Chinese Uveal Melanoma. *Precis Clin Med* **doi.org/10.1093/pcmedi/pbz021**(2019).

66. Gerstenblith, M.R., Goldstein, A.M., Fargnoli, M.C., Peris, K. & Landi, M.T. Comprehensive evaluation of allele frequency differences of MC1R variants across populations. *Hum Mutat* **28**, 495-505 (2007).
67. Eguchi, K. *et al.* An adverse pregnancy-associated outcome due to overlooked primary aldosteronism. *Intern Med* **53**, 2499-504 (2014).
68. Saner-Amigh, K. *et al.* Elevated expression of luteinizing hormone receptor in aldosterone-producing adenomas. *J Clin Endocrinol Metab* **91**, 1136-42 (2006).
69. Gagnon, N. *et al.* Genetic Characterization of GnRH/LH-Responsive Primary Aldosteronism. *J Clin Endocrinol Metab* **103**, 2926-2935 (2018).
70. Albiger, N.M. *et al.* A case of primary aldosteronism in pregnancy: do LH and GNRH receptors have a potential role in regulating aldosterone secretion? *Eur J Endocrinol* **164**, 405-12 (2011).
71. Berthon, A., Drelon, C. & Val, P. Pregnancy, Primary Aldosteronism, and Somatic CTNNB1 Mutations. *N Engl J Med* **374**, 1493-4 (2016).
72. Murtha, T.D., Carling, T. & Scholl, U.I. Pregnancy, Primary Aldosteronism, and Somatic CTNNB1 Mutations. *N Engl J Med* **374**, 1492-3 (2016).
73. Fernandes-Rosa, F.L. et al. Genetic Spectrum and Clinical Correlates of Somatic Mutations in Aldosterone-Producing Adenoma. Hypertension 54, 354-61 (2014).
74. Binder, J.X. et al. COMPARTMENTS: unification and visualization of protein subcellular localization evidence. Database (Oxford) 2014, bau012 (2014).
75. Burton, T.J. et al. Evaluation of the sensitivity and specificity of (11)C-metomidate positron emission tomography (PET)-CT for lateralizing aldosterone secretion by Conn's adenomas. J Clin Endocrinol Metab 97, 100-9 (2012).
76. Letavernier, E. et al. Blood pressure outcome of adrenalectomy in patients with primary hyperaldosteronism with or without unilateral adenoma. J Hypertens 26:1816-23 (2008).
77. Funder, J.W. et al. Case detection, diagnosis, and treatment of patients with primary aldosteronism: an endocrine society clinical practice guideline. J Clin Endocrinol Metab 93, 3266-81 (2008).
78. Tissier, F. et al. Mutations of beta-catenin in adrenocortical tumors: activation of the Wnt signaling pathway is a frequent event in both benign and malignant adrenocortical tumors. Cancer Res 65, 7622-7 (2005).
79. Akerstrom, T. et al. Comprehensive re-sequencing of adrenal aldosterone producing lesions reveal three somatic mutations near the KCNJ5 potassium channel selectivity filter. PLoS One 7, e41926 (2012).
80. De Sousa, K. et al.. Genetic, cellular, and molecular heterogeneity in adrenals with aldosterone-producing adenoma. Hypertension 75(4), 1034-44 (2020).
81. Bustin S.A. Why the need for qPCR publication guidelines?-The case for MIQE. Methods 50(4), 217-26 (2010).
82. Gomez-Sanchez, C.E. et al. Development of monoclonal antibodies against human CYP11B1 and CYP11B2. Molecular and cellular endocrinology 383(1-2), 111-7 (2014).

Acknowledgements

The CTNNB1 plasmid was a kind gift of Dr Mariann Bienz, Medical Research Council Laboratory of Molecular Biology, Cambridge. The project was funded in part by the British Heart Foundation through a Clinical Research Training Fellowship FS/19/50/34566 and PhD Studentship FS/14/75/31134; by the National Institute of Health Research (NIHR) through Efficacy and Mechanisms Evaluation Project 14/145/09 and Senior Investigator award NF-SI-0512-10052; and by Barts and the London Charity project MGU0360, all to M.J.B. The project was further funded through institutional support from INSERM, the Agence Nationale de la Recherche (ANR-15-CE14-0017-03), and the Fondation pour la Recherche Médicale (EQU201903007864) to M.C.Z. E.A.B.A. is a Royal Society-Newton Advanced Research Fellow (NA170257/FF-2018-033). R.V.T. is supported by a Wellcome Trust Investigator Award (grant number 106995/Z/15/Z) and the National Institute for Health Research (NIHR) Oxford Biomedical Research Centre Programme. C.P.C. is supported the NIHR Biomedical Research Centre at Barts and The London School of Medicine and Dentistry. The research of J.L.K., Z.T., and R.F. was supported by the National Medical Research Council and Biomedical Research Council of Singapore. Research in London and Cambridge, UK, was further supported by the NIHR Barts Cardiovascular Biomedical Research Centre (BRC), and Cambridge BRC-funded Tissue Bank. The research utilised Queen Mary University of London's Apocrita HPC facility, supported by QMUL Research-IT. http://doi.org/10.5281/zenodo.438045 . Assistance of the Endocrine Unit Laboratory of the National University of Malaysia (UKM) Medical Centre, and from Ms. Long Kha Chin and Ms. Siti Khadijah, UKM, is acknowledged.

Author Contributions

C.P.C., E.A.B.A. and M.J.B. discovered the mutations in *GNA11* and *GNAQ,* replicated by J.Z. and F.F.R. J.Z., E.A.B.A., C.P.C., F.F.R., S.B. (Boulkroun), H.S., M.C.Z., and M.J.B. conceived and designed the

subsequent experiments/analyses. C.J., A.T., H.S., E.C., G.A., X.W, E.G., L.A. S.B.2 (Backman), P.H., P.B., T.A., R.S., D.B., J.K., and F.K.F. contributed to cohort ascertainment, phenotypic characterization and recruitment. S.B.2, C.P.C., S.P., Z.T., L.M., T.A., D.G. and S.G. contributed to whole-exome/RNA sequencing production, validation, analysis and re-analysis. J.Z., F.F.R., S.B., X.W., A.T., E.A.B.A., E.C., S.G., G.A., T.A. performed targeted sequencing and RT-PCR analyses. J.Z. performed the laser capture microdissection (LCM) and genotyping of adrenal zones and biopsy punches. S.J., S.B., A.M. and J.Z. performed and F.F.R. and E.A.B.A. analysed the immunohistochemistry (IHC) staining. J.Z., S.G., A.G., K.L., and R.V.T. contributed to the plasmids construction for *GNA11* and *GNAQ*. J.Z., E.A.B.A., and G.A. performed the functional experiments on transfected H295R and primary human adrenal cells. J.Z. and S.O. undertook confocal analyses. J.Z., E.A.B.A., F.F.R., C.M., R.F., E.W., D.K., J.L.K., Z.T. and C.P.C. performed the ddPCR, WES and NGS for genotyping of adjacent adrenals regions. C.P.C., J.Z., E.A.B.A., and M.J.B. contributed to statistical analyses. E.A.B.A. and M.J.B. drafted the manuscript, for which J.Z., E.A.B.A., C.P.C., F.F.R., S.B., T.A., A.M., and M.J.B. contributed figures. C.P.C., F.F.R., S.B., M.G., V.M. and M.-C.Z. critically reviewed the text. All authors read and approved the manuscript.

Competing Interests Statement

The authors declare no competing financial interests.

Figure Legends

Figure 1

Clinical and cellular schemas showing the critical roles of GNA11/Q, and their p.Gln209 residue, in the production of aldosterone

(**a**) The renin-angiotensin-aldosterone system is superimposed on an axial PET CT image through the adrenal glands. The image is taken from the 11C-metomidate PET CT of one of the women whose unilateral (left) double-mutant aldosterone-producing adenoma (APA) was diagnosed by the scan.

The hormone-enzyme, renin, is secreted from the kidneys in response to low blood pressure or sodium (Na^+) flux. Its substrate, the protein angiotensinogen, is cleaved into an inert decapeptide, angiotensin 1 (Ang 1), which is converted on further cleavage by the angiotensin-converting-enzyme (ACE) into the octapeptide, Ang II. This is a potent vasoconstrictor and principal physiological stimulus of aldosterone production in the zona glomerulosa cells of the outer adrenal cortex. The cellular actions of Ang II is mediated by coupling of its receptor (AT1R) to inositol trisphosphate (IP_3) and intracellular calcium (Ca^{2+}) release, through a trimeric G-protein whose α subunit is either Gα11 or Gαq.

(**b**) A single-cell of a double-mutant APA, illustrating [i] similar 2D and 3D-structures of GNA11/Q and GNAS; [ii] proximity of the Q209 (GNA11/Q) or Q227 (GNAS) residue to GDP; [iii] synergism between somatic mutations of GNA11/Q and CTNNB1, upregulating luteinising hormone and human choriogonadotrophin receptor (LHCGR) expression and production of aldosterone.

The Q209 residue of Gα11 or Gαq (encoded by GNA11 or GNAQ) and analogous residue of other G-proteins are essential for GTPase activity.[17] 3D-structures for GNAQ and GNAS show the p.Gln residue in purple. Somatic or mosaic mutation of p.Gln inhibits GTPase activity and constitutively activates downstream signalling. We find that p.Gln mutation of GNA11/Q stimulates aldosterone production, and, in the adrenal, always co-exists with somatic mutation in exon 3 of CTNNB1. This prevents inactivation by phosphorylation (e.g. of p.Ser33, in purple, in the partial 3D sequence). Double-mutation of GNA11/Q and CTNNB1 induces high expression of multiple genes, including LHCGR, the Gαs/cyclic AMP coupled receptor of luteinising and pregnancy hormones.

The 3D structures of CTNNB1, GNAS, GNAQ, AT1-receptor, renin, ACE were downloaded from models 6M93, 3C14, 4QJ3, 6YV1, 2V0Z, 1O8A, respectively, at www.rcsb.org/.

Figure 2

Mutations of *GNA11/Q* Q209 increase aldosterone production in human adrenocortical cells

(**a**) Transfection of mutations of *GNA11* Q209 (Q209L, Q209P, and Q209H) into immortalized adrenocortical H295R cells stimulated aldosterone secretion (*n*=40 wells examined over 5 independent experiments, $p=1x10^{-15}$ by Kruskal-Wallis test, $\chi2(4)=105.78$).

(**b**) *CYP11B2* mRNA expression was increased in H295R cells transfected with *GNA11* mutations (*n*=12-31 biologically independent samples, $p=9x10^{-9}$ by Kruskal-Wallis test, $\chi2(4)=43.34$).

(**c**) Effect of *GNA11* mutations on aldosterone secretion in H295R cells co-transfected with either scrambled SiRNA (SiScrambled) or SiRNA targeting *CTNNB1* (SiCTNNB1) (*n*=12-20 biologically independent samples).

(**d**) Effect of *GNA11* mutations on aldosterone secretion in H295R cells in the presence of the selective β-catenin inhibitor ICG-001 (3 μM) or vehicle control (*n*=10 wells examined over 3 independent experiments).

(**e**) Cells from APA 351T, wild-type for *CTNNB1* and *GNA11*/Q (genotype presented in **Supplementary Table 2**), were transfected with either wild-type *GNA11* (WT) or *GNA11* Q209H/L only (Q209H/L) or co-transfected with either wild-type *CTNNB1* (WT + WT) or *CTNNB1* Δ45 (Δ45). Double mutations increased aldosterone secretion compared to single mutations (*n*=3 independent transfections, *p*=0.0003 by one-way ANOVA).

(**f**) Effect of *GNAQ* Q209H mutation on aldosterone secretion in H295R cells (*n*=10 wells examined over 3 independent experiments).

For box and whiskers plots (**a**, **b**, and **f**), the central line, box and whiskers indicate the median, interquartile range (IQR) and the 10^{th}-90^{th} percentile, respectively. For bar charts (**c** and **d**) and scatterplots (**e**), data are presented as mean values $\pm$ SEM.

Results for **a**, **b**, **d** and **f** are expressed as fold-change from wild-type untreated transfected cells. Results for **c** and **e** are expressed as pM of aldosterone per ug of protein.

The exact sample number (*n*) are as indicated below the x-axis. *P*-values of Dunn's multiple comparisons test are as indicated in **a** and **b**, whereas the *p*-values indicated in graph in **e** are of Bonferroni's multiple comparisons test. *P*-values indicated in **c**, **d**, and **f** are according to two-tailed Student's *t*-test.

ns, not significant.

Figure 3

High LHCGR expression in *GNA11/Q* and *CTNNB1* double mutant adrenal cells.

(**a**) *LHCGR* mRNA in 10 double mutant *CTNNB1* Mutated APAs in the discovery UK/Irish cohort was increased compared to 24 *CTNNB1* Negative APA, and 32 control adjacent adrenals (p=0.0001 by Kruskal-Wallis test, $\chi2(2)=18.09$).

(**b**) *LHCGR* mRNA in five double mutant APAs in the replication French cohort was increased compared to seven APAs with solitary *CTNNB1* mutations, nine *CTNNB1* Negative APA, and six control normal adrenals (p=0.003 by Kruskal-Wallis test, $\chi2(3)=13.70$).

(**c**) *LHCGR* mRNA in one double mutant APA in the replication Swedish cohort compared to two APAs with only *CTNNB1* mutations, 20 *CTNNB1* Negative APA, and three cortisol-producing adenomas (CPA) (p=0.08 by Kruskal-Wallis test, $\chi2(3)=6.87$).

(**d**) LHCGR protein is highly expressed in double mutant APAs that presented at times of high LH/HCG (e.g. **Patient 6** during menopause and **Patient 7** during pregnancy) compared to single *CTNNB1* mutant APAs (e.g. **Patient F11**). Scale bars, 2mm.

(**e**) mRNA of *GNA11* (green symbols, n=6), *CTNNB1* (magenta symbols, n=6), and *LHCGR* in APA 392T cells transfected with vector control (n=11), Δ45 *CTNNB1* untagged plasmid (n=11), Q209P *GNA11* GFP tagged plasmid (n=12), or co-transfected with both Δ45 *CTNNB1* and Q209P *GNA11* plasmids (n=10). *LHCGR* mRNA was increased in double mutant cells (p=0.02 by Kruskal-Wallis test, $\chi2(3)=9.78$). The central line, box and whiskers indicate the median, IQR and the 10^{th}-90^{th} percentile, respectively. Error bars presents geometric mean $\pm$ s.d.

(**f**) Immunofluorescence of GNA11 (green), CTNNB1 (magenta), and LHCGR (red), of cells transfected as in **e**. Scale bars, 50μm.

(**g**) Corrected Total Cell Fluorescence (CTCF) of LHCGR in cells transfected as in **e**-**f**. Double mutant cells had higher CTCF compared to vector control (p=0.0003 by one-way ANOVA). Exact n numbers indicated below the x-axis. Data presented as mean values $\pm$ s.e.m.

P-values of Dunn's multiple comparisons test indicated in **a**, **b**, and **e** (*, p=0.02 comparing vector and double mutant cells) and Holm-Sidak's multiple comparison test in **g**.

n, represents biologically independent samples. Squares, males. Circles, females. Open symbols, fresh-frozen/RNAlater–preserved tissues. Close symbols, FFPE tissues. Red symbols, double mutants. Blue symbols, *KCNJ5* mutants. Black symbols, *KCNJ5* wild-type.

Extended Data Figure 1

High LHCGR expression in GNA11 and CTNNB1 double mutant double mutant co-transfected primary human adrenal cells.

(**a**) APA 351T cells transfected with CTNNB1 (untagged plasmid) and GNA11 (GFP tagged plasmid) wild-type or Q209P (red boxed cell). LHCGR and CTNNB1 increased expressions were visualised same as in **Figure 3f** using the primary antibody rabbit anti-LHCGR #NLS1436 (1:200; Novus Biologicals, UK) and the primary antibody mouse anti-CTNNB1 #610154 (1:100; BD transduction Lab, USA), respectively. Scale bars, 50µm.

(**b**) Immunofluorescence of LHCGR in APA 351T were quantified using corrected total cell fluorescence (CTCF). LHCGR expression was increased in cells expressing high CTNNB1 and GNA11 Q209P (the exact number, n, of cells quantified from 2 independent experiment are as indicated below the x-axis; the *p*-values indicated are according to Kolmogorov – Smirnov statistical test). High CTNNB1 was determined as CTCF >10,000. Data are presented as mean values $\pm$ s.e.m.

Figure 4

Gene expression profiles in *GNA11*/*Q* and *CTNNB1* double mutant adrenal cells.

(**a**) Heat map representation of 362 differentially expressed genes (DEG) with large variance (log2 difference>4) among aldosterone-producing adenomas (APA) in at least one of 3 transcriptome studies (2012 microarray including patient 6[7], 2015 microarray including patient 4[26], Swedish RNAseq[19]). Each column represents the expression profile of the APA (*n*=38). Both genes and individual APA are hierarchically clustered. The unsupervised cluster analysis of samples, indicated by the bracketing above the heat map, separated the expression profiles of *GNA11*/*Q* and *CTNNB1* double mutant APAs (boxed **red**). **Yellow** and **blue** colors indicate high and low expression levels, respectively, relative to the mean (as indicated by the color scale bar).

(**b**) Zoomed image of the heat map in (a) of six interesting DEG (yellow arrow) that separated double mutant (**DM**) APAs from single mutant APAs (**SM**) and other APA genotypes. *LHCGR* (**red** arrow) and *CYP11B1* (**black** arrow) also clustered the double mutant APAs together.

(**c**) The DEG highlighted in (**b**) were investigated in double mutant APAs from the UK/Irish cohort compared to CTNNB1 Negative APAs. All, except for *C9ORF84* (which had a trend), had significantly higher mRNA expression in double mutant APAs (the *p*-values indicated are according to Kolmogorov – Smirnov statistical test).

(**d, e, f**) The DEG *TMEM132E* mRNA expression was significantly higher in double mutant APAs from the UK/Irish cohort compared to CTNNB1 Negative APAs (**d**; p=0.001 by Kolmogorov – Smirnov test), in double mutant APAs from the French cohort compared to CTNNB1 single mutant APAs (**e**; p=0.0002 by Kruskal-Wallis test, $\chi2(2)=13.01$; *p*-values of Dunn's multiple comparisons test are as indicated), and in *GNA11* Q209L transfected H295R cells compared to *GNA11* wild-type transfected cells (**f**; p=0.001 by two-tailed Student's t-test). The central line, box and whiskers indicate the median, IQR and the 10th-90th percentile, respectively. *GNA11* mRNA expression in *GNA11* Q209L and wild-type transfected cells were not significantly different.

The exact sample number (*n*), as indicated below the x-axis, represents biologically independent samples. Squares, males. Circles, females. Red symbols, double mutants. Blue symbols, *KCNJ5* mutants. Black symbols, *KCNJ5* wild-type.

Figure 5

Aldosterone synthase (CYP11B2) and 11β-hydroxylase (CYP11B1) expression in *GNA11/Q* and *CTNNB1* double mutant APAs.

(**a**) qPCR analysis of *CYP11B1* and *CYP11B2* mRNA expression found double mutant APAs to have a lower *CYP11B1*/*CYP11B2* mRNA expression ratio compared to *CTNNB1* single mutant APAs or APAs wild-type for *CTNNB1* and *GNA11/Q* (*CTNNB1*-neg APA) (p=0.00004 by Kruskal-Wallis test, $\chi2(2)=20.23$; p-values of Dunn's multiple comparisons test are as indicated). Results expressed as fold-change from *CTNNB1* wild-type APAs (*CTNNB1* Negative APA) APA. The exact sample number (n), as indicated below the x-axis, represents biologically independent samples. Squares, males. Circles, females. Red symbols, double mutants. Blue symbols, *KCNJ5* mutants. Black symbols, *KCNJ5* wild-type. Data are presented as geometric mean values $\pm$ s.d.

(**b**) Immunohistochemistry of CYP11B2 and CYP11B1 in the UK/Irish cohort using the primary antibody anti-CYP11B2 #ab168388 (1:200; Abcam, UK) and anti-CYP11B1 #MABS502, clone 80-7 (1:100; Sigma-Aldrich, USA). The histotype of high CYP11B2 protein expression and low CYP11B1 expression was apparent correlating with the low CYP11B1/CYP11B2 mRNA expression seen in (**a**). Scale bars, 2.5mm.

Figure 6

***GNA11* somatic mutations were found in the adjacent adrenals to double mutant APAs of Patient 7 (a-c) and Patient 1 (d-f).**

(**a**) gDNA from 6 different regions (R1-6) in the fresh frozen adrenal sample and the associated RNA from regions 1-3 were genotyped for *CTNNB1* and *GNA11* mutations.

(**b**) qPCR of samples in (**a**) reported a 135-151 fold lower mRNA expression level of *CYP11B2* and 16102-23987 fold lower mRNA expression level of *LHCGR* in R1 cDNA compared to R2 and R3, respectively. Differentially expressed genes (DEG) highly expressed in double mutant APAs but lowly expressed in R1 cDNA are presented in **Supplementary Figure 6a** (ii).

(**c**) Sanger sequencing of samples in (**a**) detected solitary *GNA11* Q209H mutation in R1 cDNA and double *CTNNB1* S45F and *GNA11* Q209H mutations in R2 and R3 cDNA. Interestingly, genotyping of R1 gDNA (from the exact same sample as R1 cDNA) detected a homozygous *GNA11* Q209H mutation (**Supplementary Figure 6a(i))**.

(**d**) Patient 1 was found to have hyperplastic zona glomerulosa in adrenal adjacent to double mutant APA. ZG hyperplasia was demarcated by lack of subcapsular CYP11B1 (visualised using a custom antibody). The hyperplastic ZG was CYP11B2 negative (visualised using a custom antibody) while LHCGR positive (visualised using the antibody NLS1436; 1:200; Novus Biologicals, UK). This phenotype is consistently present in the UK/Irish discovery cohort (**Supplementary Figure 5c**).

(**e**) gDNA from the hyperplastic ZG of 9 distinct regions of Patient 1's adjacent adrenal were collected systematically using segmental laser capture microdissection (LCM) of formalin-fixed paraffin embedded adrenal sections stained with cresyl violet.

(**f**) Solitary heterozygous and solitary homozygous *GNA11* Q209P somatic mutations were detected in LCM ZG gDNA collected in (**e**) from regions 1 (ZG1 gDNA) and 6 (ZG6 gDNA), respectively. ZG samples from other regions were wild-type for both *CTNNB1* and *GNA11* along with the other adrenal zones (**Supplementary Figure 6b**).

Extended Data Figure 2

***GNA11* somatic mutations were found in the adjacent adrenals to double mutant APA of Patient 6.**

(**a**) From 6 different regions (R1-5, at the edges of the adrenal cortex, R6 and APA, within the circled areas) in the formalin fixed paraffin embedded (FFPE) adjacent adrenal gland, gDNA samples of patient 6 were genotyped for *CTNNB1* and *GNA11* mutations. Immunohistochemistry of KCNJ5 and CYP11B2 were used for region selection. Scale bar, 10 mm and 50 μm as indicated.

(**b**) Sanger sequencing identified weak chromatogram peaks of *CTNNB1* G34R and *GNA11* Q209P somatic mutations in region 6 of the adjacent adrenal gland.

(**c**) Next generation sequencing confirmed the *CTNNB1* G34R and *GNA11* Q209P mutations in region 6 of the adjacent adrenal gland.

(**d**) qPCR of R1-6 and APA reported a 337-fold higher of *TMEM132E*, 38-fold higher of *CYP11B2*, 14-fold higher of *DKK1* and 10-fold higher of *LHCGR* expression in region 6 compared to region 5. Region 1-5 have similar expression of the above genes. The APA had the highest expression of *CYP11B2, TMEM132E, DKK1, LHCGR* and lowest expression of *CYP11B1* and *LGR5* compared to Region 1-6.

Table 1. Clinical, biochemical, and *GNA11/Q* genotype findings in the discovery cohort of 10 UK/Irish PA patients with *CTNNB1* mutant APAs.

Somatic mutations of *CTNNB1* and *GNA11* in the UK/Irish discovery cohort was detected in patient 1, 2, and 3 by WES of APAs from 41 PA patients. Patients 4-6 are the three previously-reported women[17], with patient 4's somatic mutation of *CTNNB1* detected in our first WES[6].

Patient ID	Gender	Age at surgery	Onset presentation	Tumor genotype		Measurements pre-adrenalectomy					Measurements post-adrenalectomy				
				CTNNB1	GNA11/Q	SBP	DBP	Plasma renin	Aldosterone	Serum potassium	SBP	DBP	Plasma renin	Aldosterone	Serum potassium
						mmHg	*mmHg*	*mU/liter*	*pmol/liter*	*mmol/liter*	*mmHg*	*mmHg*	*mU/liter*	*pmol/liter*	*mmol/liter*
					GNA11										
1	Male	12	Puberty	S45F	Q209P	180	120	<2	1,358	2.7	110	75	7	74	4.2
2	Female	35	Pregnancy	S45P	Q209P	155	85	<2	559	2.6	123	76	16	283	4.0
3	Female	20	Pregnancy	T41A	Q209H	215	120	<2	1,330	2.5	121	68	N/A	N/A	N/A
4	Female	34	Pregnancy	S33C	Q209H	190	100	<2	2,885	2.0	111	69	31	250	4.1
5	Female	26	Pregnancy	S45F	Q209H	140	86	<2	2,590	2.0	120	70	N/A	N/A	N/A
6	Female	52	Menopause	G34R	Q209P	190	100	<2	672	3.1	118	79	9.0	158	4.1
7	Female	39	Pregnancy	S45F	Q209H	160	101	<2	2,382	2.5	120	83	16.1	124	4.7
8	Female	41		S45F	Q209P	160	90	<2	480	3.2	101	65	91	236	4.5
					GNAQ										
9	Female	23	Pregnancy	G34E	Q209H	167	114	<2	2000	3.3	121	85	N/A	N/A	N/A
10	Female	26	Pregnancy	G34R	Q209L	170	110	<2	603	4.1	123	78	14	408	4.7

N/A, not available. Units of measurements pre- and post- adrenalectomy are shown in italics. Bold denotes the name of the gene (*GNA11*/*GNAQ*) in which the Q209 mutation was found.

Table 2. Clinical presentation and genotype of *GNA11/Q/S* in the APA of 17 PA patients who had *CTNNB1* mutant APAs from the replication cohorts.

Replication Cohort	Patient ID	Gender	Age PA	Hypertensive at pregnancy (Number of pregnancies)	Tumour genotype						
					CTNNB1 genotype	GNA11 Q209	GNA11 R183	GNAQ Q209	GNAQ R183	GNAS Q227	GNAS R201
French Cohort	F1	Female	29	Yes (1)	S45F	WT	WT	WT	WT	WT	WT
	F2	Male	40	-	S45P	WT	WT	WT	WT	WT	WT
	F3	Female	35	No (2)	S37C	WT	WT	WT	WT	WT	WT
	F4	Male	33	-	S45A	WT	WT	WT	WT	WT	WT
	F5	Female	43	No (1)	S45F	Q209P	WT	WT	WT	WT	WT
	F6	Female	45	Yes (2)	S45P	WT	WT	WT	WT	WT	WT
	F7	Female	55	N/A	S45P	WT	WT	WT	WT	WT	WT
	F8	Female	55	N/A	S45P	WT	WT	WT	WT	WT	WT
	F9	Female	26	Yes*(1)	S37P	WT	WT	Q209H	WT	WT	WT
	F10	Female	51	Yes (1)	S45P	Q209H	WT	WT	WT	WT	WT
	F11	Male	36	-	S45P	WT	WT	WT	WT	WT	WT
	F12	Female	56	No (10)	D32Y	Q209H	WT	WT	WT	WT	WT
	F13	Female	56	No (0)	S45Y	WT	WT	WT	WT	WT	WT
	F14	Female	17	No# (0)	G34V	WT	WT	Q209H	WT	WT	WT
Swedish Cohort	S1	Female	55	Yes†(2)	S45P	WT	WT	Q209H	WT	WT	WT
	S2	Female	59	N/A	S45P	WT	WT	WT	WT	WT	WT
	S3	Female	26	N/A	S37F	WT	WT	WT	WT	WT	WT

N/A, not available. WT, wild-type. *, pre-eclampsia. #, hypertensive at puberty. †, onset at age 24 year old preceding first pregnancy.

The 13 *CTNNB1* mutant APAs from the French replication cohort were detected through screening 198 primary aldosteronism patients for *CTNNB1* mutations. For part of the patients included in the French cohort, the genetic screening of known aldosterone-driving mutations in ion-channel/transporter genes was previously performed[23]. The *GNAQ* mutation in the *CTNNB1* mutant APA from the Swedish replication cohort were detected through reanalysis of a published RNA Sequencing dataset of 15 APAs with known aldosterone-driving mutations of which 3 were *CTNNB1* mutant APAs[20]. All of the *GNA11/Q* mutations in the *CTNNB1* mutant APAs from the UK/Irish discovery cohort and the French replication cohort were verified by Sanger Sequencing (**Supplementary Figure S1**). In the Swedish replication cohort, RNA sequencing reported the 3 *CTNNB1* mutant APAs to be wild-type for all known ion-channel/transporter gene mutations (*ATP1A1*, *ATP2B3*, *CACNA1D*, and *KCNJ5*).

METHODS

Patient cohorts

All patients were confirmed to have PA by raised aldosterone/renin ratio, positive confirmatory tests and lateralisation studies (CT/PET CT[75], MRI and AVS) according to the institutional protocols at the various centres and in accordance with the Endocrine Society guidelines[76,77]. All patients gave written informed consent for genetic and clinical investigation according to local ethics committee guideline (Cambridgeshire Research Ethics Committee for Addenbrooke's Hospital, University of Cambridge or the Cambridge East Research Ethics Committee for St Bartholomew's Hospital, Queen Mary University of London for the UK cohort; Assistance Publique-Hôpitaux de Paris Research Ethics Committee for the French cohort; Regional Ethical Review Board in Uppsala for the Swedish cohort).

UK/Irish cohort. The seven patients with double-mutations of *CTNNB1* and *GNA11* were among 117 UK/Irish patients who were investigated at St Bartholomew's Hospital, London or Addenbrooke's Hospital, Cambridge, or whose operative specimen was received for investigation, during the period 2004 to 2017.

French cohort. Patients with PA were recruited between 1999 and 2016 within the COMETE (COrtico- et MEdullo-surrénale, les Tumeurs Endocrines) network (COMETE-Hôpital Européen Georges Pompidou protocol authorization CPP 2012-A00508-35). 198 patients were screened for *CTNNB1* mutations. For part of the patients included in this study, the genetic screening of mutations in *KCNJ5, ATP1A1, CACNA1D* and *ATP2B3* was previously described[73,78].

Swedish cohort. 15 tumours were selected from a previously documented international cohort[19,79]. Adrenal specimens were collected from 348 patients from centres in Sweden, Germany, France and Australia.

Whole exome sequencing (WES)

Whole exome sequencing of 40 pairs of APAs and adjacent adrenal from UK patients was conducted in the Barts and London Genome Centre, and the Cardiovascular Research Institute of the University of Singapore, with overlap of eight pairs of samples, and previously genotyped controls (n=3 in each centre/institute) as validation of sensitivity (not included in analysis). The 41st APA was analysed together with germline DNA from blood processed commercially by GATC Biotech, Germany. MuTect2 analysis was conducted in order to identify adrenocortical genes with somatic mutations, predicted by Sorting Intolerant from Tolerant (SIFT) and Polymorphism Phenotyping (PolyPhen)-2 to be functional. Candidate mutations were confirmed by Sanger sequencing of DNA from fresh samples of the APA, and sought in other previously genotyped APAs that were not included in the WES.

Quality control of whole exome sequencing (WES) samples. Genomic DNA of samples were quality assessed by gel electrophoresis, Agilent 2200 Tapestation and Genomic DNA screentape (Agilent Technologies, Waldbronn, Germany), or as per GATC Biotech standard protocol. Samples with low degradation and a majority of high molecular weight were taken forward for WES.

WES of patient 1. WES using the Illumina HiSeq 2000 Sequencer was conducted on DNA extracted from the APA along with the paired germline DNA extracted from the venous blood (samples processed commercially by GATC Biotech, Germany). WES samples were prepared as an Illumina sequencing library and the sequencing libraries were enriched using the Agilent SureSelectXT Human All Exon V6 Kit. The captured libraries were sequenced and downstream analysis conducted as described below.

WES of patient 2. WES using the Illumina NextSeq 500 Sequencer was conducted on genomic DNA extracted from APAs from 21 PA patients along with paired adjacent normal adrenal and APAs from 3 PA patients with known genotype (as sensitivity controls). 50 ng of each DNA sample was processed using the Nextera Rapid Capture Enrichment kit, with the Coding Exome Oligo (CEX) pool. Tagmented DNA was assessed using the Agilent 2200 Tapestation in conjunction with the HSD1000 screentape. All samples showed expected fragmentation profiles with an average fragment size of 300bp. Enriched libraries were validated using the Agilent 2200 Tapestation in conjunction with the D1000 screentape. Equimolar

amounts of each sample library were pooled together for sequencing which was carried out using the llumina NextSeq®500 high-output kit.

WES of patient 3. WES using the Illumina Hiseq 2500 sequencer was conducted on genomic DNA extracted from 27 APAs along with paired adjacent normal adrenal and 3 APAs with known genotype (as sensitivity controls). 1ug of genomic DNA was fragmented using sonication (Covaris, S220), optimized to give a distribution of 200-500 base pairs that was verified using a 2100 Bioanalyzer (Agilent, G2939BA). Library preparation was carried out using Kapa DNA HTP Library Preparation Kit (KAPA Biosystems, 07 138 008 001). Hybridization of adapter ligated DNA was performed at 47°C, for 64 to 72 hours, to a biotin-labelled probe included in the Nimblegen SeqCap EZ Human Exome Kit (Roche, 06465692001). Libraries were sequenced using the Illumina Hiseq 2500 sequencing system and paired-end 101bp reads were generated for analysis with a 100x coverage per sample.

WES data analysis. Variant calling was performed using Burrows-Wheeler Aligner (BWA) v. 0.7.12 (for 341T) or v. 0.7.15 to align raw reads in the FASTQ files to human reference genome GRCh37. The alignments were sorted and marked for PCR duplicates using Picard Tools software v.1.119 (for 341T) or v. 1.7. This was followed by base quality score recalibration (BQSR) using the genome analysis toolkit (GATK) for tuning the quality scores to reflect higher accuracy of base qualities. For 341T, ContEst from GATK was used to calculate cross-sample contamination between samples, using blood as the “normal” versus each of the APA samples. A panel of normals was created from the blood sample of the boy using dbSNP and COSMIC as reference. In order to enrich the panel of normals, we utilize WES of 11 other blood samples, all pre-processed using the same protocol as described above. Resulting BAMs were analysed with GATK MuTect v.2 software to identify somatic variants. Normal and tumour pairs were analysed together when available. For tumour only samples, the MuTect tumour-only algorithm was used. The contamination estimates derived from ContEst, and the dbSNP, COSMIC, the blood sample and the panel of normals were used as resources in the input parameters to filter variants observed in the germline samples. Single Nucleotide Polymorphisms, with a threshold coverage of at least 10 reads on the

respective nucleotide, were assessed. Oncotator was used to annotate the variants passing the filters [http://www.broadinstitute.org/oncotator].

Re-analysis of RNAseq data of Swedish cohort

RNA sequencing previously described in Backman et al (2019)[20] was used for variant identification and analysed for gene expression differentiation.

RNA-sequencing variant detection. RNA-sequencing variant detection was performed following the recommendations on the GATK workflow for RNA seq variant discovery. RNA seq reads were aligned to the UCSC hg19 reference genome using the STAR 2-pass method for sensitive novel junction discovery. Picard tools software [picard-tools-1.119] was then used to sort and mark PCR duplicates on the alignments. The SplitNCigarReads function from GATK was used to reformat alignments, by splitting reads into exon segments, and to reassign reads with good mapping quality into a GATK format. We performed an indel realignment step followed by the quality score recalibration protocol. Variants were called using the HaplotypeCaller from GATK using the '–dontUseSoftClippedBases' parameter and setting the minimum phred-scaled confidence threshold to 20 (-stand_call_conf 20.0). The following hard filters were applied to the called variants: '-window 35 -cluster 3 -filterName FS -filter "FS > 30.0" -filter Name QD -filter "QD < 2.0"'. Variant annotation was performed using ANNOVAR.

Gene expression differentiation of double mutant APA compared to single CTNNB1 mutant only APA. Gene expression differentiation of the three samples with the *CTNNB1* mutation was performed as follows. RNA seq fastq files were pseudo-aligned to the human *GRCh37* cDNA reference sequences from ENSEMBL using kallisto v0.46.0. Transcript abundance was quantified using the kallisto 'quant' function with default settings. Gene expression analysis was performed with DESeq2 [v1.24.0]. Genes with less than 10 reads were removed from further analysis. Dispersion estimates and size factors were calculated using all 15 samples, with gender as a covariate in the design matrix. The two single-mutation samples were then compared to the sample with a double-mutation.

Sanger sequencing of *CTNNB1* and *GNA11/Q/S*

Laser capture microdissection (LCM) of adrenal zones. Freshly sectioned 10 um FFPE adrenal sections of patient 1 were used for LCM. Serial adrenal sections were fixed and rehydrated in ethanol then stained by cresyl violet (Sigma-Aldrich, USA) for 1 min. The sections were then dehydrated in ethanol and cleaned in Histo-clear II (AGTC Bioproducts Ltd, UK). After fixing and staining the adrenal sections, ZG cells were collected by LCM technique using a Zeiss PALM Microbeam laser microdissection system (Carl Zeiss Microscopy, USA) with PALMRobo v4.3 software according to the manufacturer's instructions. All the pooled ZG LCM samples collected from the same area of adrenal sections were then stored at -20°C until RNA and gDNA extraction.

***Nucleic acid extraction*.** Genomic DNA (gDNA) from fresh frozen/RNAlater solution–preserved tissue samples was extracted using Reliaprep™ gDNA Tissue miniprep system (Promega, USA). gDNA from FFPE samples collected by laser capture microdissection (LCM) were extracted using Arcturus® PicoPure® DNA Extraction Kit (Applied Biosystems™, USA). gDNA of blood from patient 1 and patient 7 were extracted using Nucleon™ BACC3 Genomic DNA Extraction Kit (GE Healthcare Life Sciences, UK) according to manufacturer's recommendation.

For the UK/Irish cohort, total DNA-free RNA was isolated from fresh frozen/RNAlater solution–preserved samples using TRIzol (Ambion Life Technologies, Carlsbad CA) and PureLink® RNA Mini Kit (Invitrogen™, USA) according to manufacturer's recommendation. The PureLink® DNase Set was used in combination to remove DNA from RNA (Invitrogen, USA) by on-column digestion. If the fresh frozen/RNAlater solution–preserved samples were not available, total RNA and gDNA were extracted from FFPE tissue samples blocks using AllPrep DNA/RNA FFPE Kit (Qiagen, USA) according to manufacturer's recommendation (FFPE extracted DNA/RNA is reported when used). This kit is also used on fresh frozen samples when RNA and gDNA from the same sample were required. Total RNA from FFPE samples collected by Laser capture microdissection (LCM) were extracted by Arcturus™ Paradise™ Plus RNA Extraction and Isolation Kit (Applied Biosystems™, USA) in combination with the PureLink® DNase Set, according to manufacturer's

recommendation. After extraction reverse transcription was performed using the High Capacity RNA-to-cDNA kit (Fisher Scientific, USA) according to manufacturer's instructions. The cDNA was purified by DNAclear™ Purification Kit (Invitrogen™, USA).

For the French cohort, total RNA was extracted using Janke and Kunkel's Ultra-Turrax T25 (IKA technologies, Staufen DE) in Trizol reagent (Ambion Life Technologies, Carlsbad CA) according to the manufacturer's recommendations. After deoxyribonuclease I treatment (Life Technologies, Calsbad CA), 500 ng of total RNA were retro-transcribed (iScript reverse transcriptase, Biorad, Hercules, CA).

PCR and sequencing* of *CTNNB1* and *GNA11/Q/S. Primers used for *CTNNB1*, *GNA11*, *GNAQ* and *GNAS* amplification in gDNA and cDNA samples are described in **Supplementary Table 5** and **Supplementary Table 6** or as previously described[17,73]. For UK/Irish cohort, PCR was performed on 100 ng of DNA in a final volume of 20 µl reaction using AmpliTaq Gold™ Fast PCR Master Mix (Thermo Fisher, USA) according to manufacturer's instructions. Sanger sequencing of PCR products was performed using LIGHTRUN Tube sequencing service from Eurofins (Germany). For French cohort, PCR was performed on 100 ng of DNA in a final volume of 25 µl containing 400 nM of each primer, 200 µM deoxynucleotide triphosphate and 1.25 U Taq DNA Polymerase (Sigma-Aldrich, USA). Sanger sequencing of PCR products was performed using the Big Dye TM Terminator v3.1 Cycle Sequencing Kit (Applied Biosystems, USA) on an ABI Prism 3700 DNA Analyzer (Applied Biosystems, USA). Sanger Sequencing alignment was performed using GATC Viewer 1.00 or BioEdit version 7.2.5.

Droplet digital PCR (ddPCR) of *GNA11/Q*

Specific droplet digital PCR (ddPCR) assays for GNA11 (c.627 A>C, c.627 A>T, and c.626A>C) and GNAQ (c.627A>C and c.627A>T) mutation detection were designed on the Bio-Rad's Digital Assay Site. Each ddPCR reaction mixture (20 µL) contained 45 ng of DNA template, 1 µL of 20X WT (HEX) and mutant (FAM) assays, 4U of restriction enzyme HindIII (New England Biolabs), and 10 µL of 2X Bio-Rad ddPCR Supermix.

The reaction mixture was mixed with 70 µL Bio-Rad droplet generator oil and partitioned into 15,000–20,000 droplets by using the QX-100 droplet generator (Bio-Rad), and transferred to a 96-well PCR reaction plate. PCR conditions were 10 min at 95°C, 40 cycles of denaturation for 30 s at 94°C and extension for 60 s at 57°C with ramp rate of 2.5°C.s-1, followed by 10 min at 98°C. The plate was then transferred to the QX-100 droplet reader (Bio-Rad). QuantaSoft software version 1.3.2.0 (Bio-Rad) was used to quantify the copies of target DNA. The ratio of positive HEX and positive FAM events was used to identify the presence and the proportion of target mutations.

NGS targeted sequencing of *CTNNB1* and *GNA11/Q/S*

NGS at the French centre: Immunohistochemistry-guided next generation sequencing (CYP11B2 IHC-guided NGS) was performed as previously described[80]. Before DNA extraction from FFPE tissue, APA was identified by CYP11B2 IHC and the areas of interest were delimited and isolated for DNA extraction by scraping unstained FFPE sections guided by the CYP11B2 IHC slide using a scalpel under a Wild Heerbrugg or Olympus microscope. DNA was extracted from FFPE sections using the AllPrep DNA/RNA FFPE kit (Qiagen). NGS was performed using an amplicon based NGS kit on an Illumina MiSeq sequencer as previously described[80].

NGS at the British centre: Assays were designed using Primer3 and 5'tagged with Fluidigm TSP sequences to allow barcoding and adapter addition. Samples were PCR amplified with FastStart High Fidelity (Roche) with cycling conditions (95C, 2 minutes, 35 cycles (95C, 30 secs, 55C, 30 secs, 72C 30 secs), 72C for 5 mins on an MJ tetrad MJ225. PCRs were checks on 2% agarose gel. 1ml of a 1 in 100 dilution of PCR product was used in a second round of PCRs to add Barcodes and Illumina adapters, 95C, 10 minutes, 15 cycles (95C, 30 secs, 60C, 30 secs, 72C 30 secs) 72C for 3 mins on an MJ tetrad MJ225. Products were quantified by Qubit and loaded onto an Illumina NextSeq 500 to generate in excess of 1000X 75bp paired end reads. Reads were aligned to human hg38 using BWA and BAM files visualised in IGV.

Whole Exome Sequencing for validation

WES was performed for validation for some samples listed in Table S4. Using the Illumina Hiseq 4000 sequencer was conducted on genomic DNA. 1ug of genomic DNA was fragmented using sonication (Covaris, S220), optimized to give a distribution of 200-500 base pairs that was verified using a 2100 Bioanalyzer (Agilent, G2939BA). Library preparation was carried out using Kapa DNA HTP Library Preparation Kit (KAPA Biosystems, 07 138 008 001). Hybridization of adapter ligated DNA was performed at 47°C, for 64 to 72 hours, to a biotin-labelled probe included in the Nimblegen SeqCap EZ Human Exome Kit (Roche, 06465692001). Libraries were sequenced using the Illumina Hiseq 4000 sequencing system and paired-end 150bp reads were generated for analysis with a 200x coverage per sample. Exome data was analyzed using GATK v3.7 with the human_g1k_v37_decoy as reference genome. Annotation of variants was performed using annovar (version 10-24-2019) and in-house pipelines.

Functional analyses in human adrenocortical cells

Construction of wild-type and mutant vectors. *GNA11* wild-type and Q209L plasmids was kindly given by Prof. Rajesh V. Thakker from the University of Oxford, constructed in a pBI-CMV2 vector. *CTNNB1* wild-type and del45 (*CTNNB1* Δ45) plasmids were kindly given by Prof. Mariann Bienz from the University of Cambridge, constructed in a pcDNA3 vector. *GNA11* Q209H, P and *CTNNB1* S45F were generated using the NEB Q5® Site-Directed Mutagenesis Kit (New England Biolabs, UK) using the following primers in **Supplementary Table 7** according to the manufacturer's recommendation.

Functional experiments on transfected H295R and primary human adrenal cells. The human adrenocortical carcinoma cell line, H295R, and primary human adrenal cells were cultured as previously described[16]. H295R cells and primary human adrenal cells were transfected with pBI-CMV2 empty vector, *GNA11* wild-type, *GNA11* Q209H/L/P plasmids, with/or without the co-transfection of *CTNNB1* wild-type, *CTNNB1* Δ45/S45F plasmids by electroporation using the Neon™ Transfection System 10/100 µL Kit (Invitrogen™, USA).

For H295R cells, 48h after transfection, the culture medium was replaced with serum free medium with or without 10 nM angiotensin II (Ang II) or 3 or 10 µM of the CTNNB1 inhibitor, ICG-001(AdooQ BioScience,

USA). Supernatant was collected for aldosterone measurement after 24 h and cells were harvested for mRNA expression analysis and protein quantification. For primary adrenal cells, supernatant was collected for aldosterone measurement at 24, 27 (+3), 30 (+6) and 48 (+24) hours post-transfection and cells were harvested for mRNA expression analysis and protein quantification at the last timepoint (48 h post-electroporation). All cells harvested for mRNA expression analysis was kept at -80°C in trizol until batch extraction of nucleic acid and protein.

Aldosterone and cortisol measurement. Aldosterone secretion of primary human adrenal cells was measured using the Homogeneous Time Resolved Fluorescence (HTRF®) Aldosterone competitive assay (Cisbio, France) according to manufacturer's recommendation. Aldosterone secretion of H295R cells was measured on the IDS-iSYS Automated System (Immunodiagnostic Systems, Germany). The cortisol levels were measured using ECLIA-Technology (Cobas e411, Roche, Germany) and immunoassay for the in vitro quantitative determination of cortisol (#06687733 190, Roche, Germany). Aldosterone and cortisol results were normalized by protein amount estimated by Pierce BCA Protein Assay Kit (Thermo Fisher Scientific, USA) according to manufacturer's recommendation.

RT-qPCR analyses

RT-qPCR analysis of APAs from the UK/Irish Cohort and adrenocortical cells. mRNA expression of genes of interest was quantified using commercially available TaqMan gene expression probes (Thermo Fisher Scientific, USA) listed in **Supplementary Table 8**. The RT-qPCR was performed using the C1000 Touch Thermal Cycler machine (Bio-Rad, USA) according to manufacturer's recommendation. Results were analysed using the $2^{-\Delta\Delta CT}$ method using the housekeeping 18S rRNA (Thermo Fisher Scientific, USA) for normalisation.

RT-qPCR analysis of APAs from the French Cohort. Primers used for *LHCGR, CYP11B1* and *CYP11B2* RT-qPCR are described in **Supplementary Table 9**. RT-qPCR was performed using SsoAdvanced Universal SYBR Green Supermix (Biorad, USA) on a Biorad C1000 touch thermal cycler (CFX96 Real Time System) according to the manufacturer's instructions. Normalization for RNA quantity and reverse transcriptase

efficiency was performed against three reference genes (geometric mean of the expression of Ribosomal *18S* RNA, *GAPDH* and *HPRT*, primers are described in **Supplementary Table 9**), in accordance with the MIQE guidelines[81]. Quantification was performed using the standard curve method. Standard curves were generated using serial dilutions from a cDNA pool of all samples. Fold change over control adrenals excised from patients who had undergone enlarged nephrectomies for renal carcinoma (*LHCGR* RT-qPCR) and over non-*CTNNB1* mutated APA (*CYP11B1* and *CYP11B2* RT-qPCR) were then calculated.

Protein expression analyses

Immunohistochemistry (IHC). The primary antibodies used for IHC are as follows: anti-LHCGR #NLS1436 (1:200; Novus Biological, USA), anti-CYP11B1 (1:100) and anti-CYP11B2 (1:100) gifted by Prof. Celso E. Gomez-Sanchez[82], two commercial anti-CYP11B2 #ab168388 (1:200; Abcam, UK) and #MABS1251 (1:2500; Sigma-Aldrich, USA), and one commercial anti-CYP11B1 #MABS502 (1:100; Sigma-Aldrich, USA). The secondary antibodies used in the IHC are as follows: affinity purified goat anti-rabbit antibody for LHCGR antibody (1:400; Vector laboratories, USA), affinity purified goat anti-mouse antibody for CYP11B2 antibody (1:400; Vector Laboratories, USA), and affinity purified rabbit anti rat antibody for CYP11B1 antibody (1:400; Vector laboratories, Burlingame, USA).

Immunofluorescence (IFC). 48h after electroporation, transfected H295R and primary human adrenal cells were processed for IFC as previously described[16]. Cells were incubated with anti-LHCGR #NLS1436 (1:200; Novus Biologicals, UK) and anti-CTNNB1 #610154 (1:100; BD transduction Lab, USA) at room temperature for 1 hour and then with goat anti-rabbit IgG (H+L) cross-adsorbed secondary antibody, Alexa Fluor 568 (A-11011, 1:1000; Invitrogen, USA) and goat-anti-mouse IgG (H+L) cross-adsorbed secondary antibody, Alexa Fluor 647 (A-21235, 1:1000; Invitrogen, USA) at room temperature for 1 hour. Immunofluorescence was visualized using a Zeiss LSM 710 (for ADR351T and 357T)/880 (for ADR392T) confocal microscopes. A second set of primary antibodies, a combination of anti-LHCGR #NBP2-52504 (1:100; Novus Biologicals, UK) and anti-CTNNB1 #71-2700 (1:100; Thermo Fisher Scientific, USA) was used for validation of first set of primary antibodies used. For the second set of primary antibodies, Alexa Fluor

405 (A-31553, 1:1000; Invitrogen, USA)/ Alexa Fluor 647 (A-21235, 1:1000; Invitrogen, USA) and Alexa Fluor 568 (A-11011, 1:1000; Invitrogen, USA) were used as the secondary antibodies. Quantification of immunofluorescence was performed using (Fiji Is Just) ImageJ v1.52e Java 1.8.0_66 as published online by Fitzpatrick, M. (2014) (Measuring cell fluorescence using ImageJ. *The Open Lab Book. https://theolb. readthedocs. io/en/latest/imaging/measuring-cell-fluorescence-using-imagej. Html).* Cells successfully transfected with Δ45 CTNNB1 was defined based on having a corrected total cell fluorescence (CTCF) for CTNNB1 >100,000.

Data Availability Statement

Source data for Figure 1B-E, 1G, and 2Ei are provided with the paper. The raw RNASeq dataset analysed to generate Figure 3A and 3B, and **Supplementary Figure 3** and **Supplementary Figure 4** is available upon requests to the Science for Life Laboratory Data Centre through the DOI link https://doi.org/10.17044/NBIS/G000007. Regulations by the service provider may make access technically restricted to PIs at Swedish organizations. The microarray datasets analysed to generate Figure 3A and 3B, is deposited in the Gene Expression Omnibus database (GSE64957) or is available from the corresponding author on reasonable request. All other raw data that support the findings of this study are available from the corresponding author upon reasonable request.

Statistical Analysis

All parametric data are presented as mean ± s.e.m. For non-parametric data, results were presented as median + 95% Confidence Interval or as geometric mean ± 95% Confidence Interval (for qPCR data only). For parametric data, two-tailed Student's t-test, and one-way or two-way ANOVA statistical tests were performed depending on the grouping factors. Kolmogorov-Smirnov test (when comparing 2 groups) or Kruskal-Wallis test (when comparing >2 groups) was used for non-parametric data. Tests for normality/lognormality and adjustment for multiple comparisons were performed. All the analysis was performed using GraphPad Prism software (Version 8.3.0 and version 9) or Microsoft Excel v.2016 (for Student's t-test). *P*-values lower than 0.05 were considered statistically significant.

Extended Data Figure 1 (a-b)

APA 351T cells transfected with *CTNNB1* (untagged plasmid) and *GNA11* (GFP tagged plasmid) wild-type or Q209P.

a.

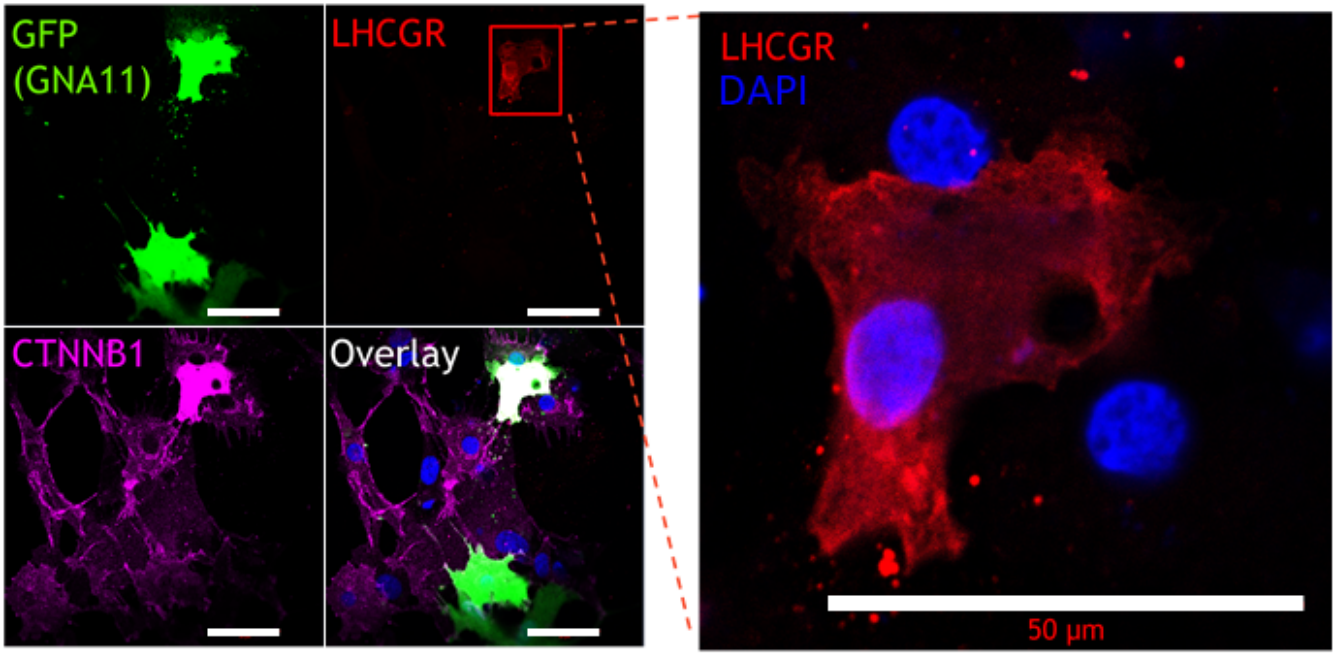

b.

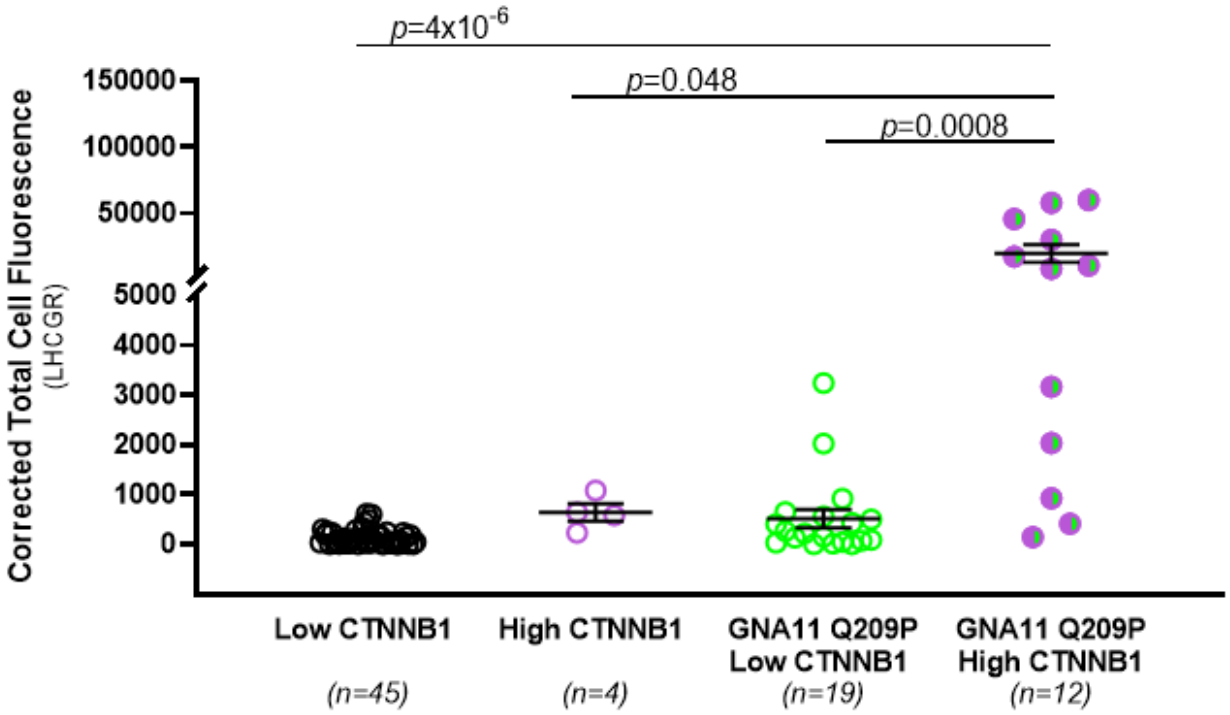

Extended Data Figure 2 (a-d)

***GNA11* somatic mutations were found in the adjacent adrenal to double mutant APA of Patient 6.**

a.

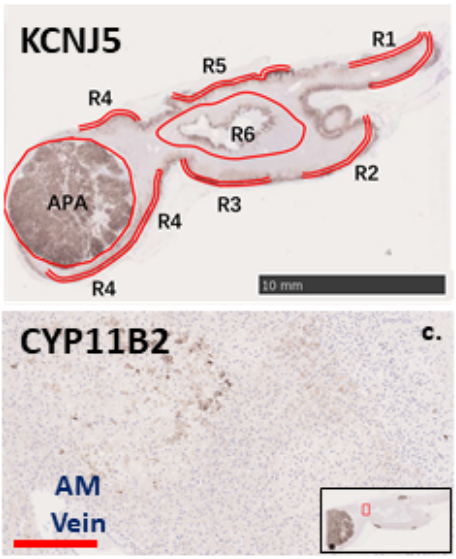

b.

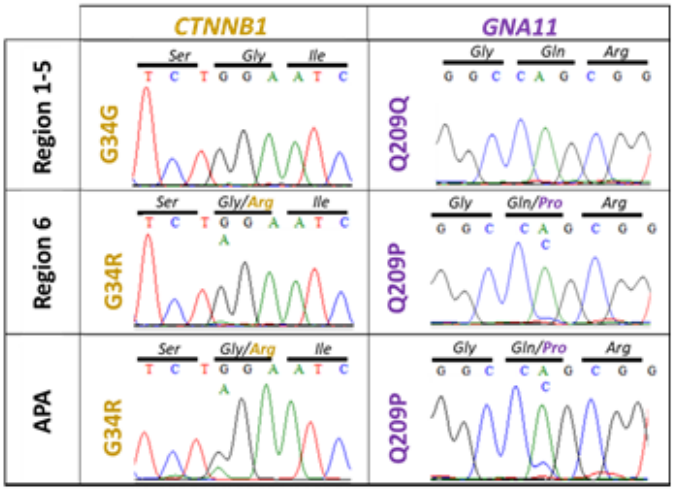

c.

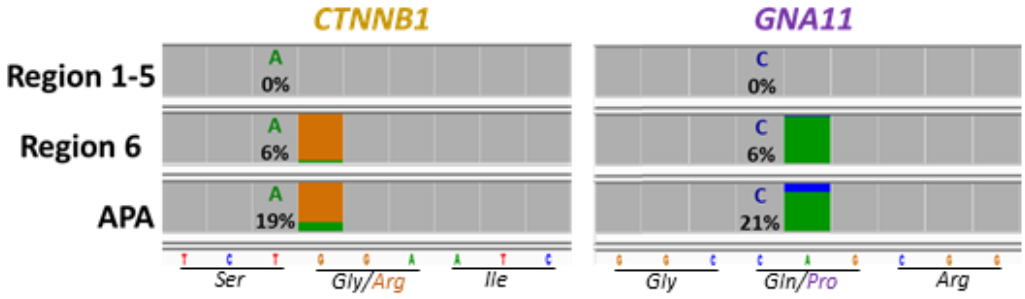

d.

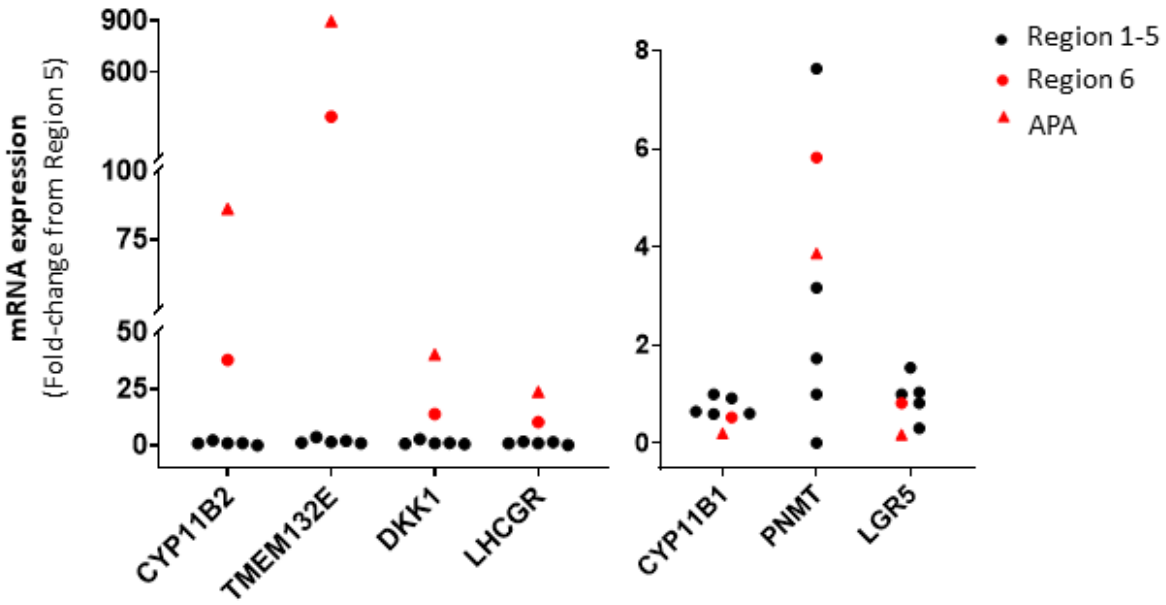

Figure 1 (a-b)

Clinical (a) and cellular (b) schemas showing the critical roles of GNA11/Q, and their p.Gln209 residue, in the production of aldosterone.

a.

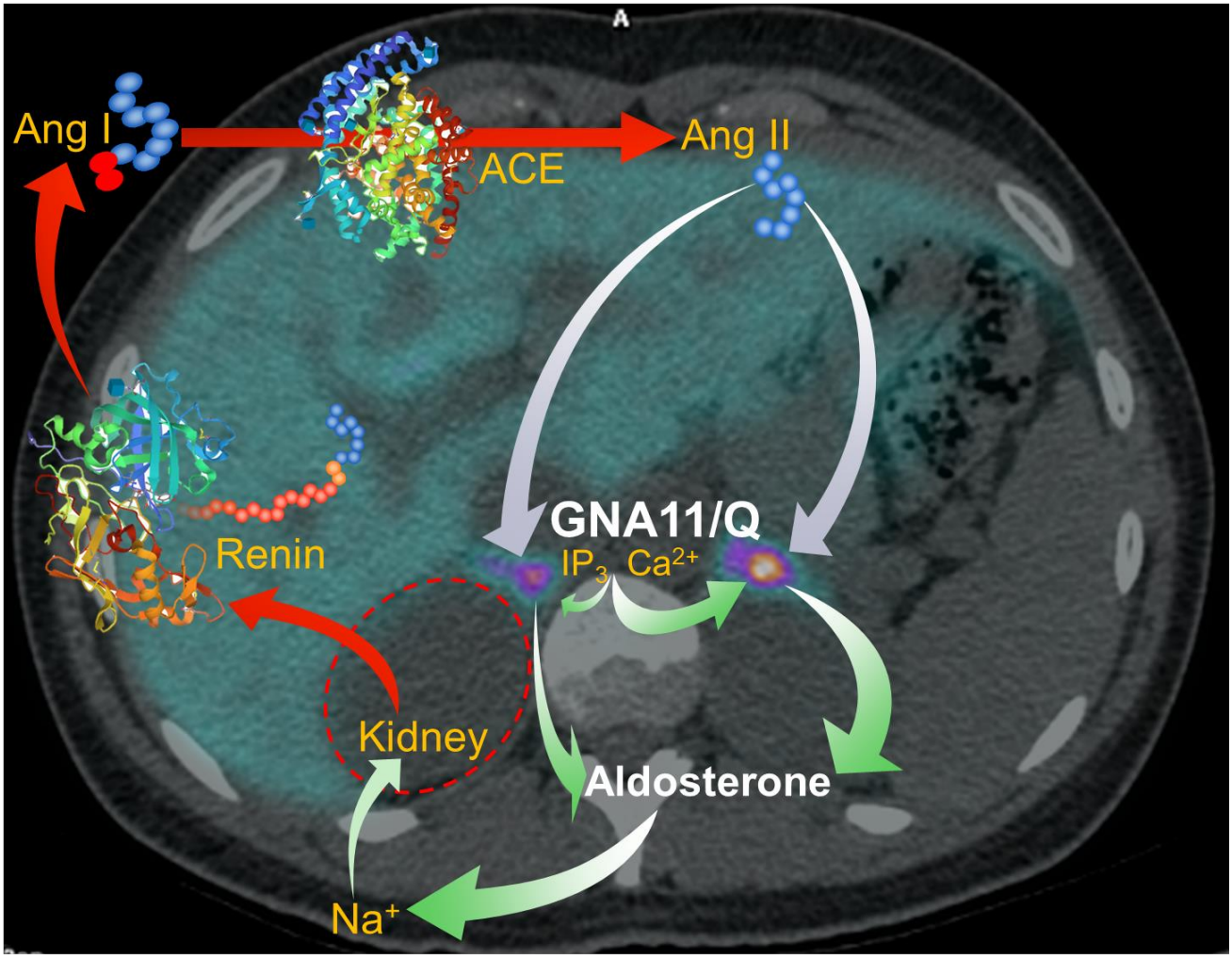

b.

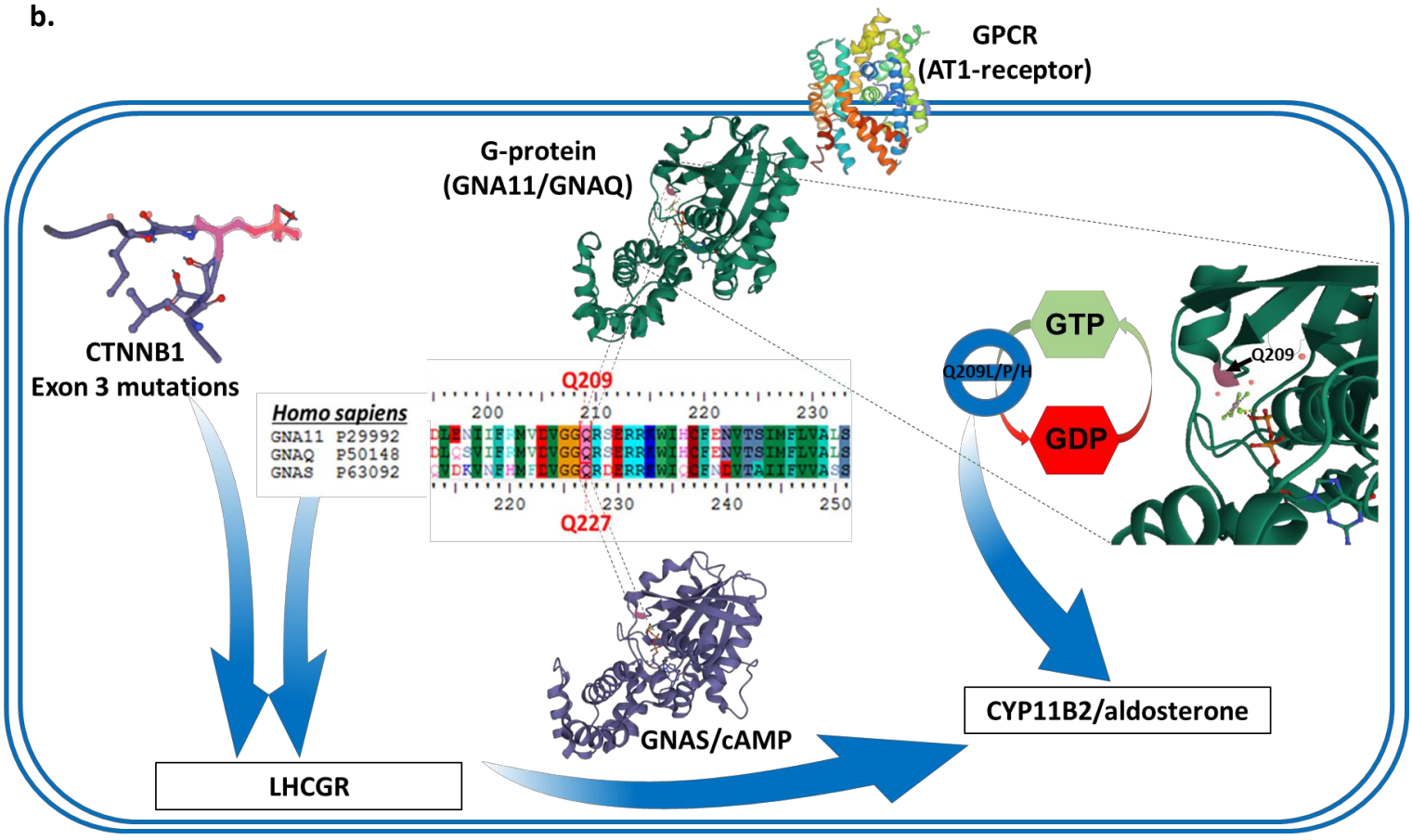

Figure 2 (a-f)

Mutations of *GNA11/Q* Q209 increase aldosterone production in human adrenocortical cells.

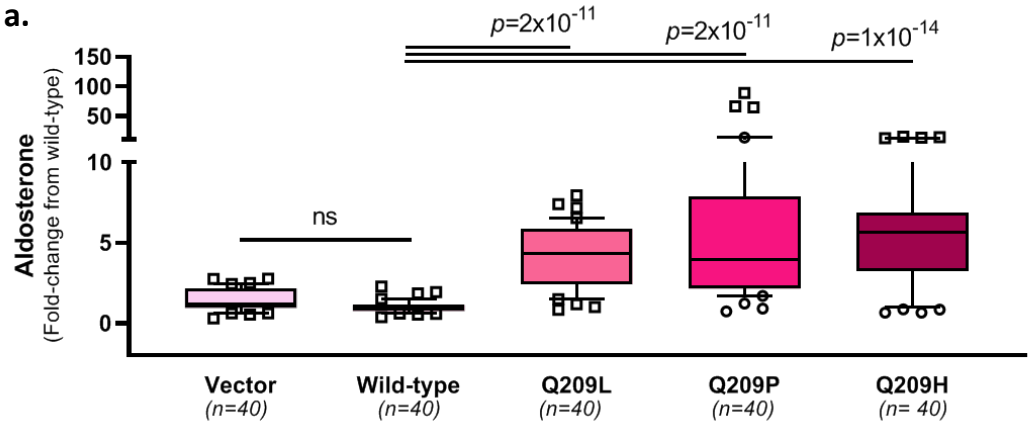

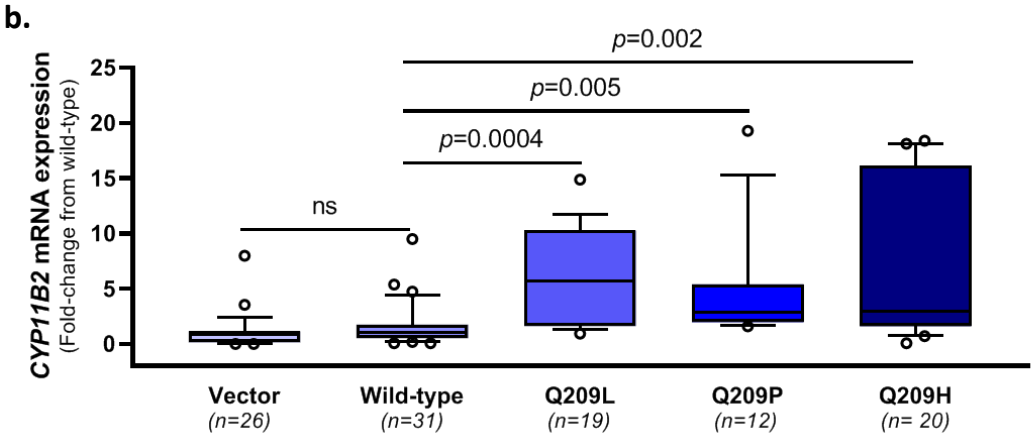

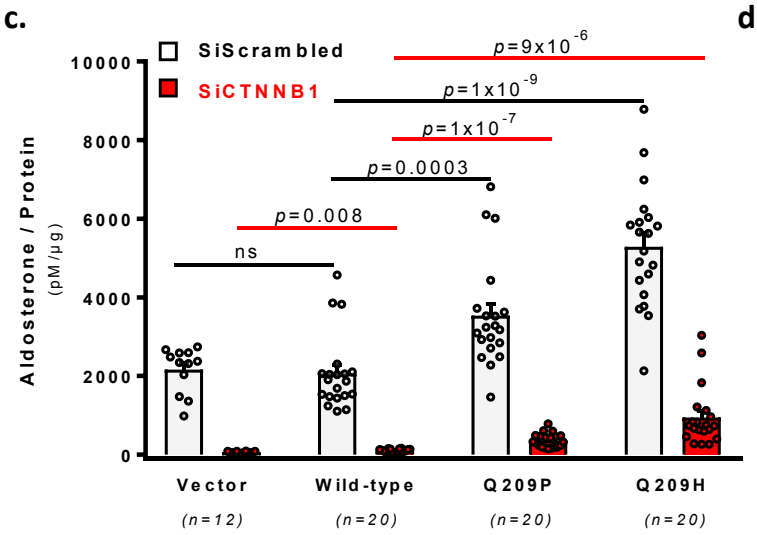

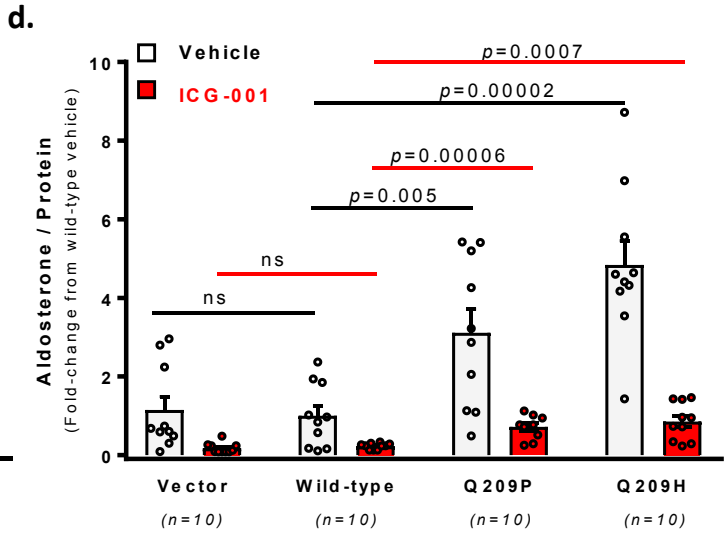

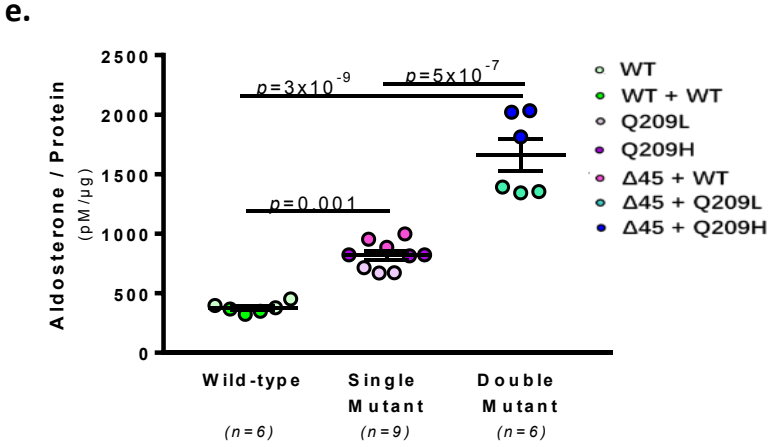

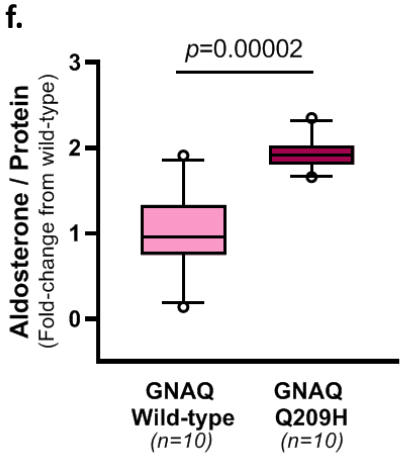

Figure 3 (a-g)

High LHCGR expression in *GNA11/Q* and *CTNNB1* double mutant aldosterone-producing adenomas (APAs) and double mutant co-transfected primary human adrenal cells.

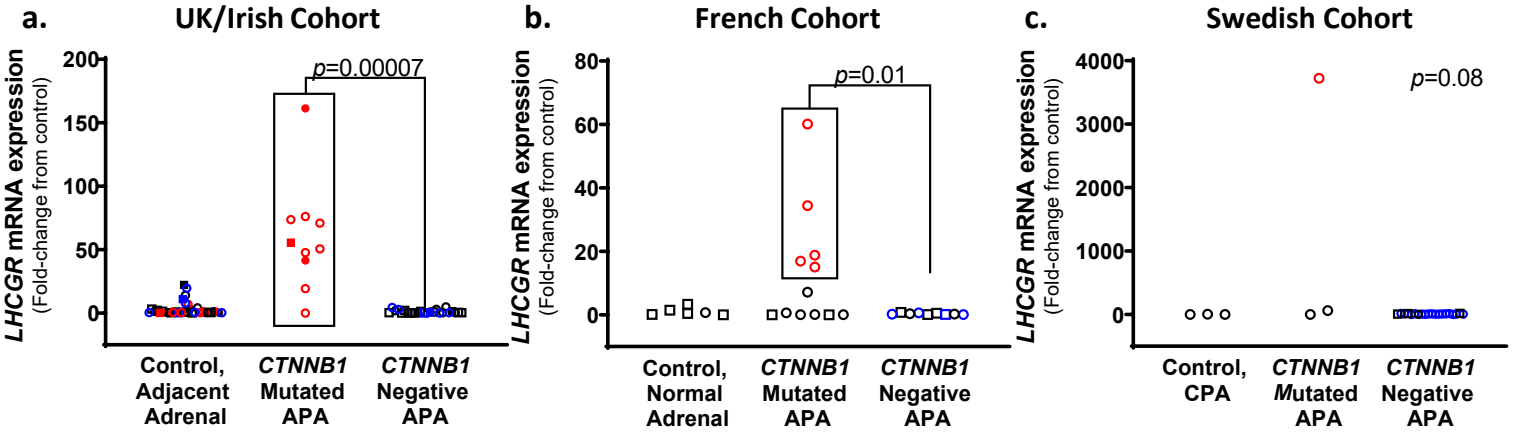

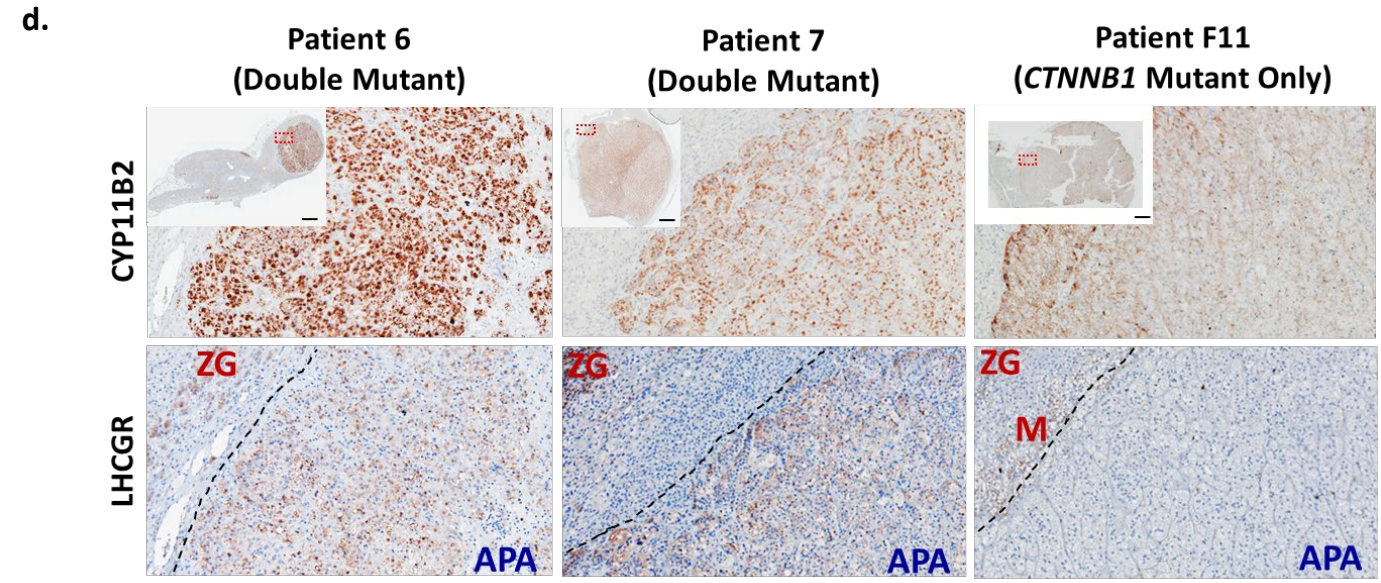

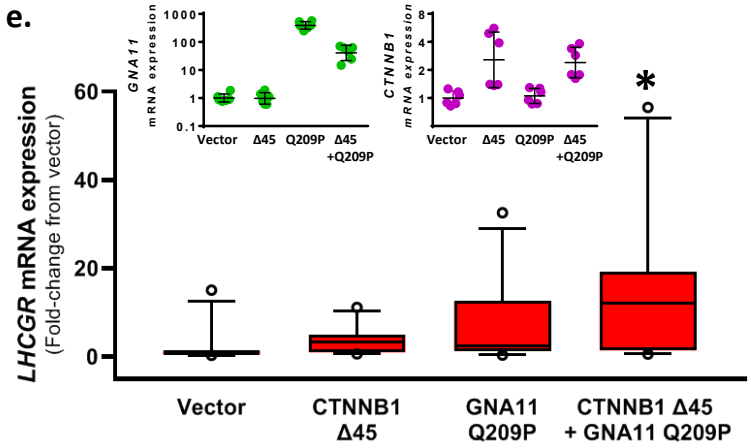

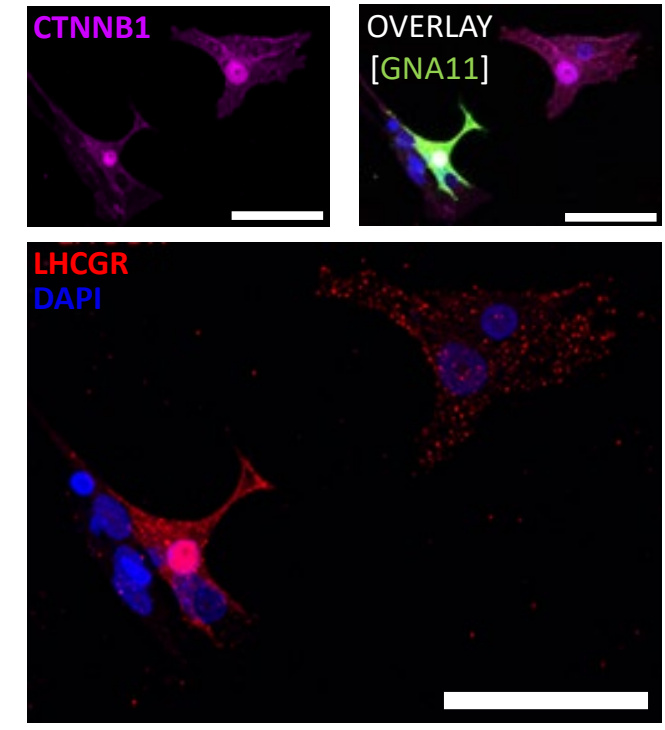

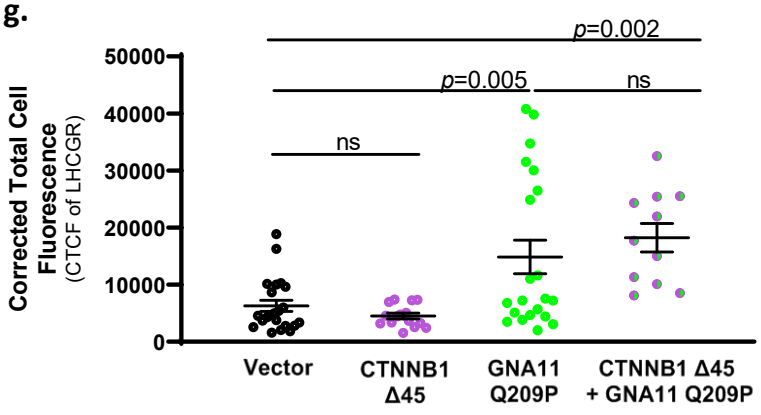

Figure 4 (a-f)

Gene expression profiles in *GNA11/Q* and *CTNNB1* double mutant adrenal cells.

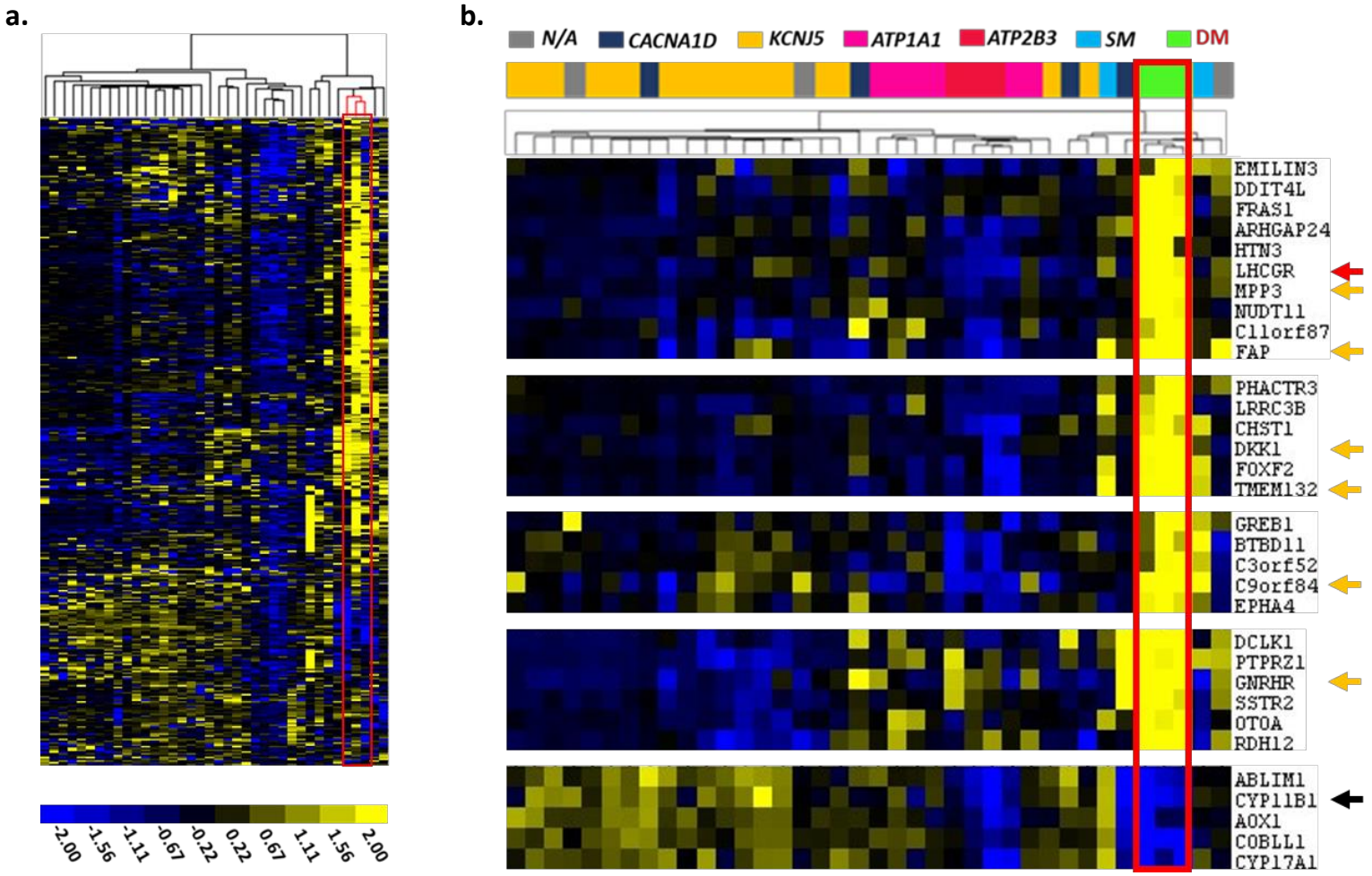

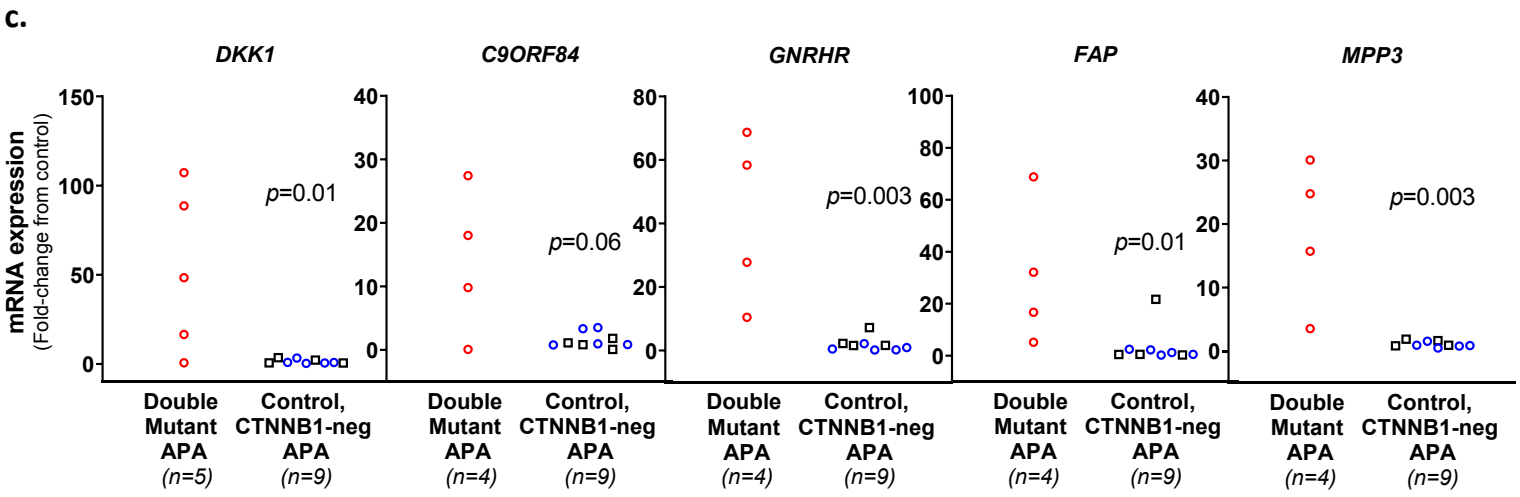

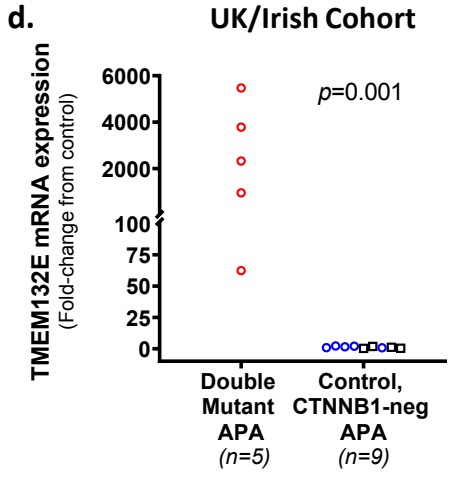

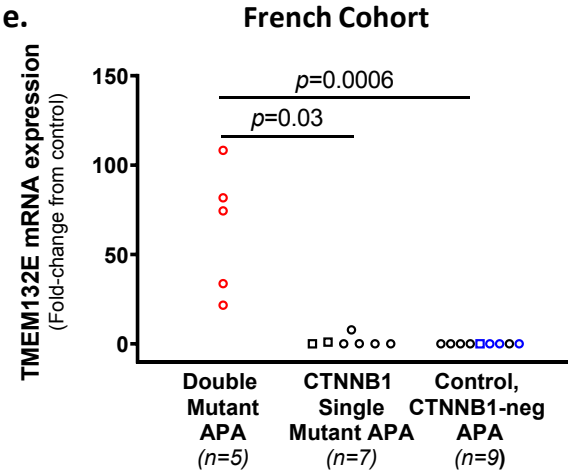

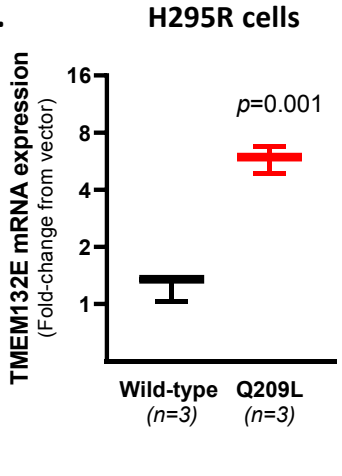

Figure 5 (a-b)

Aldosterone synthase (CYP11B2) and 11β-hydroxylase (CYP11B1) expression in *GNA11/Q and CTNNB1* double mutant APAs.

a.

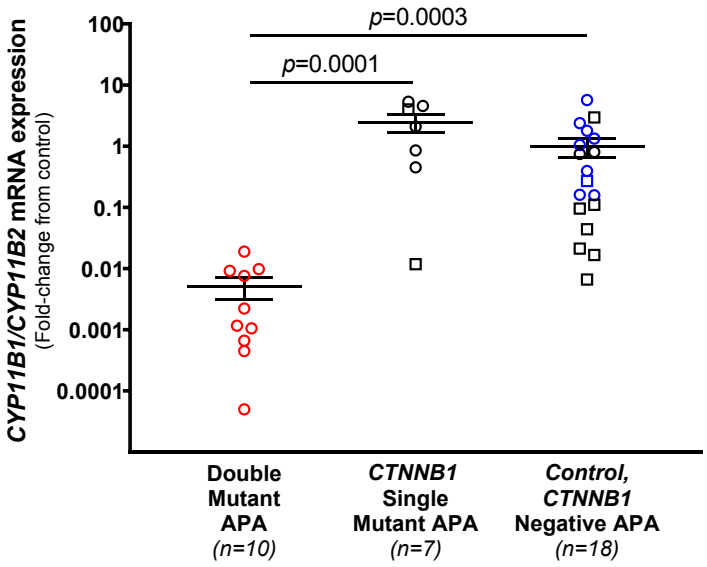

b.

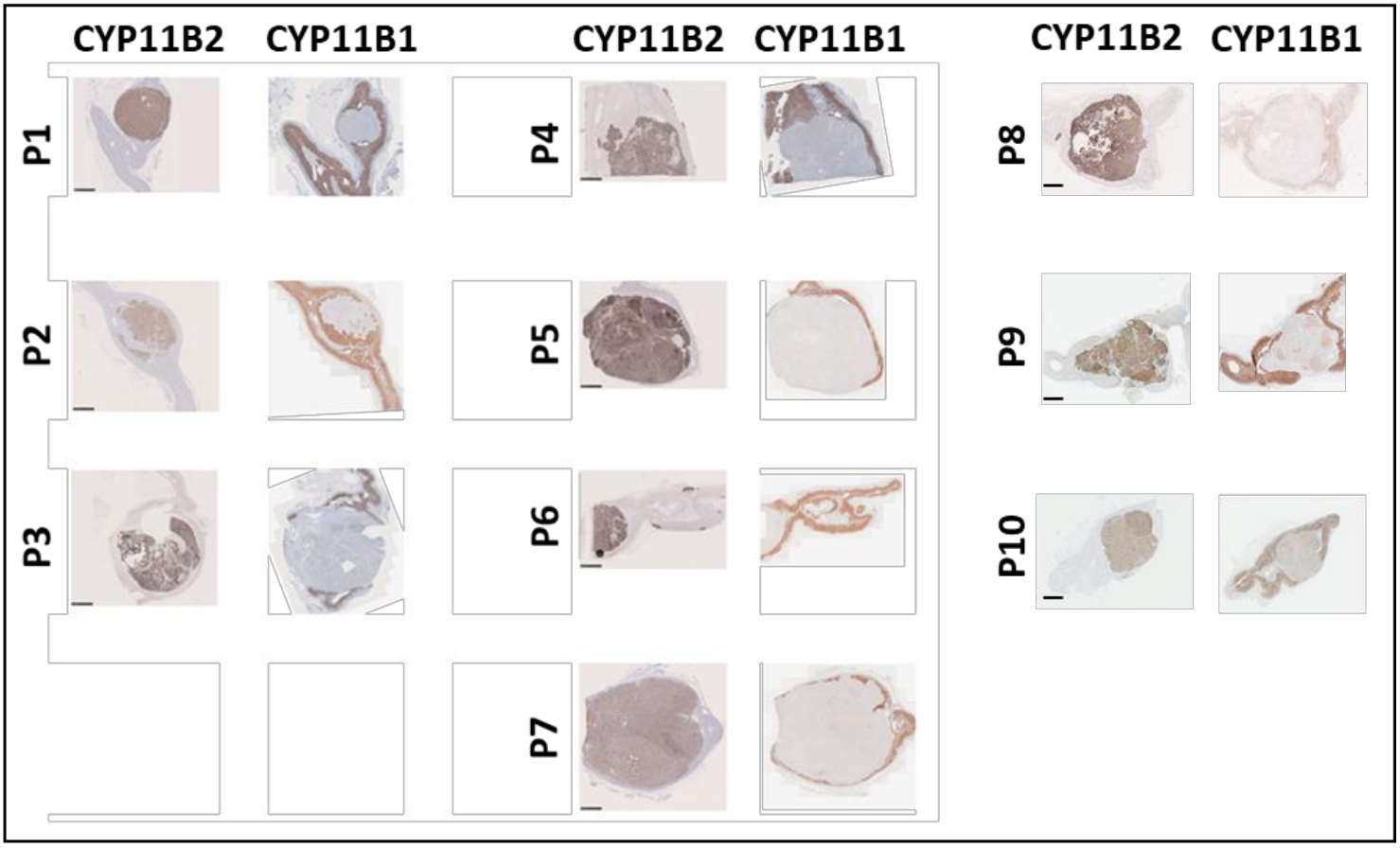

Figure 6 (a-f)

***GNA11* somatic mutations were found in the adjacent adrenals to double mutant APAs of Patient 7 (a-c) and Patient 1 (d-f).**